European Journal of Mechanics A/Solids 34 (2012) 102–119

Contents lists available at SciVerse ScienceDirect

European Journal of Mechanics A/Solids

journal homepage: www.elsevier.com/locate/ejmsol

Refined shell model for the linear analysis of isotropic and composite elastic structures

S. Brischetto [a,*], O. Polit [b], E. Carrera [a]

[a] Department of Mechanical and Aerospace Engineering, Politecnico di Torino, Corso Duca degli Abruzzi 24, 10129 Torino, Italy
[b] Laboratoire Energétique Mécanique Electromagnétisme, Université Paris Ouest Nanterre La Défense, Paris, France

ARTICLE INFO

Article history:
Received 19 July 2010
Accepted 30 August 2011
Available online 12 November 2011

Keywords:
Shell finite element
Nine components model
Composite structures
Refined theory
Shear locking
Membrane locking
Poisson locking

ABSTRACT

A refined finite element shell model has been developed in this work using an eight-nodes element with nine degrees of freedom for each node. This model enhances the classical shell approaches by including the transverse normal strain. The three displacement components are quadratically expanded in the thickness direction, therefore the transverse shear and normal strains effects are included in such a model making it suitable for thin and thick multilayered composite structures. The transverse normal strain is linear in the thickness direction z and the related shell theory is free from Poisson locking. Finite element locking mechanisms (shear and membrane locking) have been opportunely corrected: good convergence rate has been shown for the considered shell problems (with various geometries, thickness ratios and stacking layer sequences). No shear correction factors are requested.

1. Introduction

In Ramm 1986 shell structures are defined as the primadonna of structures because their behavior is difficult to analyze and they show sensitivity to geometry, support and loading conditions: numerous shell finite elements have been proposed and yet there is a consensus that there are still difficulties in analyzing general shell structures (see the review article by Bischoff et al. 2004). Also, it is difficult to identify which shell elements are the most effective elements currently available, and how to arrive at more efficient shell analysis procedures. In the considerations made in Chapelle and Bathe 1998, it is clear as the presently available finite element schemes for shell analysis are quite well for certain shell problems but they could not properly work for other problems. A shell model is an effective finite element scheme when it is applicable to both categories of shell behavior (namely, the membrane-dominated and bending-dominated cases) and the rate of convergence in either case should be optimal and independent of the shell thickness: typical shear and membrane locking problems. Although the first plate bending element has been introduced in 1961 (MacNeal, 1998), elements which are adequate for general shell analysis only became available in the 1970s. In MacNeal 1998, the author has outlined the chronology of plate and shell elements development remarking the importance of research on the design of plate and shell elements continues to this day. Bischoff and Ramm 2000 have outlined the importance of the development of higher order plate and shell models. These models are able to approximately represent three-dimensional effects, while pertaining the efficiency of a two-dimensional formulation. Especially, they give the possibility to use unmodified, complete three-dimensional material laws within shell analysis, and this is a further major motivation for the development of such models. Babuska and Li 1991 have defined the main requirements to obtain hierarchic models for plates. One of the first 7-parameter shell model has been given by Büchter and Ramm 1992 and it considers the thickness stretch of the shell by including a linear varying thickness stretch as extra variable. In fact, in conventional shell formulations, such as 3- or 5-parameters or even 6-parameters theories, a condensation of the constitutive law is required in order to avoid a significant error due to the assumption of a linear transverse displacement field across the thickness (Büchter et al., 1994). This means that the normal stress in the thickness direction has to either vanish or be constant. In general, these extra constraints cannot be satisfied explicitly or they lead to elaborate strain expressions. This phenomenon (it is not a numerical phenomenon as shear and membrane locking) has been defined as Poisson thickness locking in the 90's, and it has recently been investigated in Carrera and Brischetto (2008a,b) for plate and shell geometries, respectively: when the kinematic model is incoherent

* Corresponding author. Tel.: +39 (0) 11 564 6813; fax: +39 (0) 11 564 6899.
E-mail address: salvatore.brischetto@polito.it (S. Brischetto).

0997-7538/$ – see front matter © 2011 Published by Elsevier Masson SAS.
doi:10.1016/j.euromechsol.2011.08.008

with the physical constitutive relations, Poisson locking appears. In order to avoid Poisson locking the transverse displacement must be at least quadratically varying in the thickness direction, this means transverse normal strain at least linear in the thickness direction and three-dimensional constitutive equations can be applied. In the case of classical plate/shell theories, the transverse displacement is constant or linear in the thickness direction (zero or constant transverse normal strain) and the reduced constitutive equations must be applied (rearranging them by imposing zero transverse normal stress) (Carrera and Brischetto, 2008a,b). A possibility to remove the Poisson locking effect without increasing the number of degrees of freedom on the structural level has been proposed by Büchter and Ramm 1992, where the strain field of the element is enriched by an additional linear component ε_{33} of the thickness strain. This extra strain is introduced in the sense of a hybrid-mixed formulation by the Enhanced Assumed Strain (EAS) method. Bischoff and Ramm 1997 have proposed a 7-parameter model which considers a linear varying thickness stretch as extra variable, and then an equivalent possibility where a linear expansion in the thickness direction for the in-plane displacement components and a quadratic expansion in the thickness direction for the transverse displacement have been employed. Both these formulation are free of Poisson locking.

By referring to Carrera's Unified Formulation (CUF) (Carrera, 2003), the shell model proposed in the present paper has a quadratic thickness expansion for each displacement component allowing 9 parameters or degrees of freedom for each node. In the framework of CUF several refined plate/shell theories are possible, the 9 parameter theory chosen for this application is enough to avoid the Poisson locking phenomenon (it permits to use three-dimensional constitutive equations) and to correctly describe the behavior of orthotropic and/or moderately thick structures. The proposed model is a refinement and an improvement of the classical degenerative approach presented by Huang and Hinton 1986. Efficiency, generality and simplicity of the use of degenerative approaches have ensured the continued popularity of degenerated shell elements. The basic assumptions employed in classical degenerated shell elements are: – a general curved shell element which has nodes only at the mid-surface; – the stress in the thickness direction is assumed to be equal to zero; – the element displacement field is expressed in terms of three displacements of the mid-surface and two rotations of the mid-surface normal, and in terms of appropriate shape functions. The original degenerated shell element performs reasonably well for moderately thick shell situations. However, for thin shells when full integration is used to evaluate the stiffness matrix, overstiff solutions are often produced due to shear and membrane locking. Shear and membrane locking are the two most important numerical phenomena for shell elements: if a refinement of the mesh is time consuming to contrast them, alternative methods must be proposed in order to correct the overstiff phenomena. In the proposed model the zero transverse normal strain assumption is removed and the basic idea of the degenerative approach is used but with the inclusion of the transverse normal strain. A critical survey of the degenerated shell elements has been proposed by Parisch 1979, the elements are very accurate for both thick and thin plates and shells, and the shear and membrane locking can be contrasted by a reduced integration technique applied only to the membrane and shear stiffness and not to the whole stiffness matrix. The efficiency of the degenerative approach proposed in Huang and Hinton 1986 is also confirmed by its extension to plates and shells with variable thickness values and several boundary conditions (Afonso and Hinton, 1995).

The degenerated approach proposed in this paper considers nine degrees of freedom in each node and the general curved shell element has nodes only in the mid-surface even if the transverse

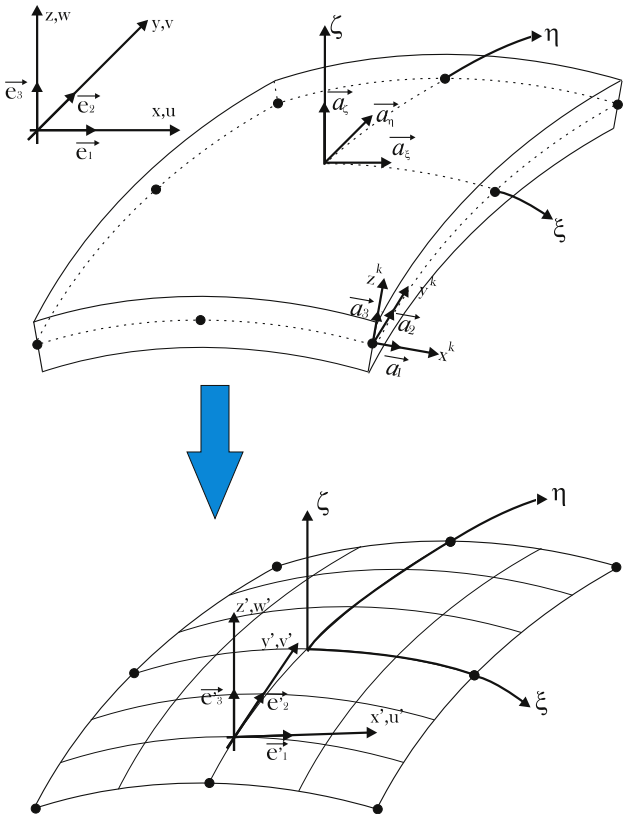

Fig. 1. Employed reference systems in the nine components kinematic model for the eight-nodes shell element (9P-8N).

normal strain is linear in the thickness direction. The model is called 9P-8N because an 8-nodes element is considered with 9 degrees of freedom per node (quadratic thickness expansion for each displacement component). Shear and membrane locking corrections are applied as proposed in Polit 1992 and Polit 2008: the stiffness matrix (that of classical isoparametric approach) is partially modified in the parts concerning the transverse shear strains and the in-plane strains which do not tend toward zero in the case of small thickness. Therefore both shear and membrane locking appears as an excessive stiffness value. In the open literature other methods are proposed in order to correct the shear and membrane locking, one of the most powerful is the mixed interpolation of tensorial components approach (MITC) as proposed in Chapelle et al. 2003 and Lee and Bathe 2005. For the same aim Kulikov and Plotnikova 2002 have used the Hu-Washizu mixed variational principle. Shear locking and curvature thickness locking have been treated using the assumed natural strain (ANS) method in Vu-Quoc and Tan 2003, where element is based on the mixed Fraeijs de Veubeke-Hu-Washizu (FHW) variational principle leading to a novel enhancing strain tensor (EAS method) that renders the computation particularly efficient, with improved in-plane and out-of-plane bending behavior (Poisson thickness locking). In Vu-Quoc and Tan 2003, an optimal combination of the ANS method and the minimal number of EAS parameters has been given.

The main idea of the 9P-8N model is: shell models based on Kirchhoff hypothesis (Kirchhoff, 1850) are suitable when the structure is thin and homogeneous because these conditions permits to respect the hypothesis of zero transverse normal strain and zero transverse shear strains. A refinement of Kirchhoff models is given by those theories based on Reissner–Mindlin (Reissner,

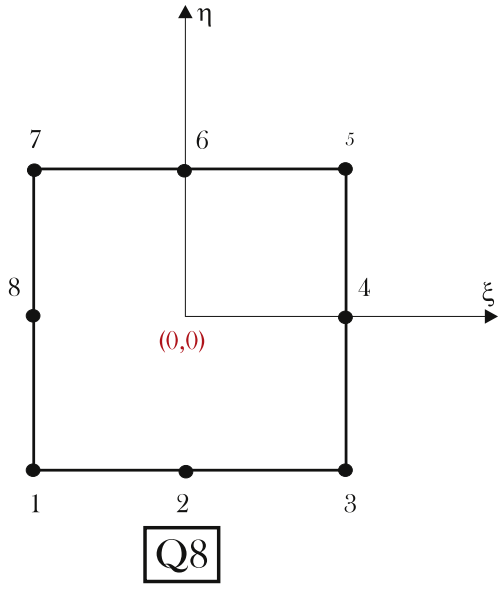

Fig. 2. Eight-nodes element (Q8) for the finite element approximation.

1945), (Mindlin, 1951) hypothesis where the transverse shear rigidity is not infinite and the transverse shear strains are not zero, in this case orthotropic structures can be investigated with good approximation because of the coupling between shear and axial strains. A possible refinement of Reissner-Mindlin models has been given by Reddy 1984: however the inextensibility of transverse normal remains, so transverse displacement w is constant in the thickness direction z. When the hypothesis of zero transverse normal strain remains, this limitation becomes evident in the case of moderately thick structures. A large amount of shell models, given in the open literature, are based on Reissner-Mindlin theory or they are a refinement of this idea, so the condition of constant transverse displacement remains and such models give good results for homogeneous and orthotropic/composite structures, but they exhibit some difficulties for moderately thick plates and shells. Dau et al. 2004 have proposed an enriched kinematic for in-plane displacements, this model satisfies the continuity requirements for multilayered/sandwich shell structures but exhibits some difficulties for thick structures because the transverse displacement remains constant in the thickness direction. The same authors extended this model to non-linear analysis in Dau et al. 2006. The flat shell element proposed by Batoz et al. 2000 is based on Kirchhoff theory and uses a 4-nodes element with 4 degrees of freedom for each node (three displacements and a rotation). This flat element has been successfully applied for the linear analysis of isotropic thin plates and shells. An interesting shell theory for the non-linear analysis has been given by Parisch 1995. A quadrilateral shell element is considered and only displacements are employed as degrees of freedom. They are located at nodes on the outer surfaces and one degree of freedom at the middle surface. This last degree of freedom is eliminated on element level, so that the elements have the same layout as the equivalent brick elements but with a better behavior in bending and stress resultants, and they are cheaper with respect to computational effort. For composite shells the element proposed in Bouabdallah and Batoz 1996 is based on a cylindrical shell finite element, which uses a first-order shear deformation theory (Reissner-Mindlin hypothesis). The stiffeners are curved beam elements based on Timoshenko and Saint-Venant assumptions for bending and torsion respectively. The two elements are developed in a cylindrical coordinate system and their stiffness matrices result from a hybrid-mixed formulation where the element assumed stress field is such that exact equilibrium equations are satisfied. The elements are free of membrane and shear locking with correct satisfaction of rigid body motions. An other element based on Reissner-Mindlin hypothesis is that proposed by Heppler and Hansen 1986 for thick and deep shells. An interesting comparison between several shell theories has been proposed by Touratier and Faye 1995, the proposed kinematics has constant transverse displacement and for in-plane displacements a function f depending on the thickness coordinate is added. This function permits to obtain Kirchhoff theory, Reissner-Mindlin theory and Reddy theory, and finally when it equals a certain sine function gives the proposed model. The proposed model is efficient with respect to classical theories and no shear correction factor is requested. Kulikov 2001 and Kulikov and Carrera, 2008 have confirmed the importance of the inclusion of transverse shear and transverse normal effects in shell models developed for multilayered anisotropic shells.

The model 9P-8N has been preliminary validated for thin isotropic plates (clamped and simply supported conditions) and for the well-known isotropic pinched cylinder, in order to verify that the element is free of shear and membrane locking and that it obtains the analytical results. Then the importance of such a refinement model has been demonstrated by considering

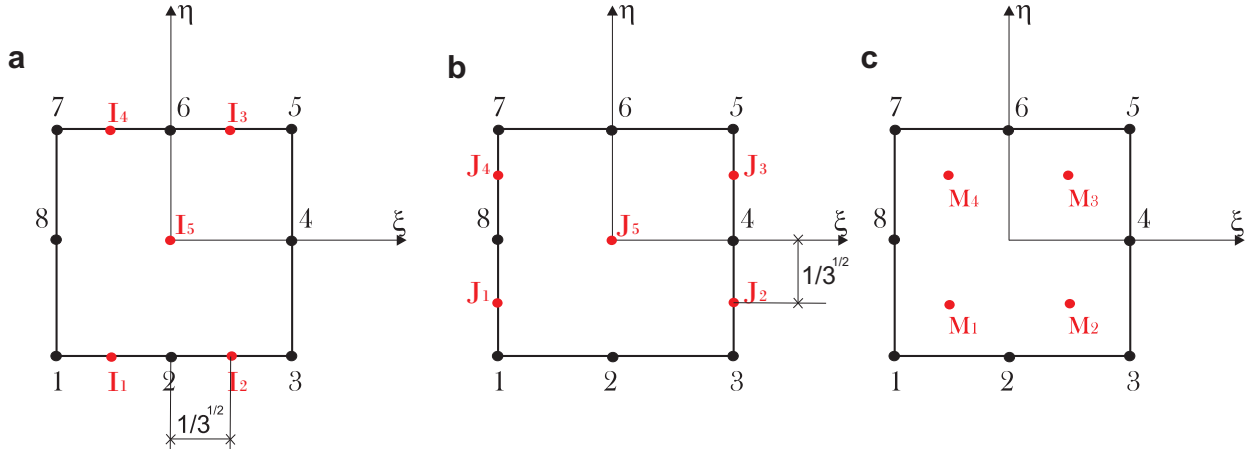

Fig. 3. Shear and membrane locking corrections: points *I* and *J* employed for the transverse shear strains and for the in-plane normal strains (a and b). Points M employed for the in-plane shear strains (c).

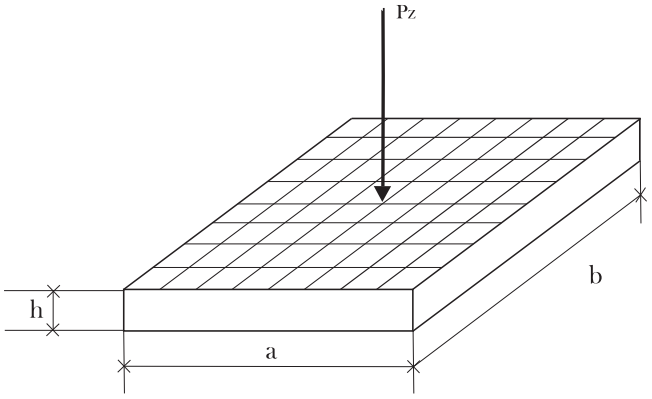

Fig. 4. Square plate with concentrated load. Simply supported or clamped edges. One-layered and multilayered isotropic/composite configurations.

moderately thick and thick isotropic and composite structures: in these cases the transverse shear and normal effects are much more evident.

2. Employed reference systems for a degenerative shell approach

The proposed model is a refinement of the classical degenerative shell approach given by Huang and Hinton 1986. In classical degenerated shell elements, a general curved shell element which has nodes only at the mid-surface is considered, the stress in the thickness direction is assumed to be equal to zero and the element displacement field is expressed in terms of three displacements of the mid-surface and two rotations of the mid-surface normal. In 9P-8N model (9 parameters for each node for an 8-nodes shell element) only the first assumption remains, in fact a quadratically transverse displacement through-the-thickness is assumed which permits to consider transverse normal strain and transverse normal stress different from zero. By considering the 8-nodes shell element employed to develop the proposed new model, four different coordinate systems can be defined (see Fig. 1):

- The global reference system is a rectilinear orthogonal system considered in the space where the shell is situated. The three coordinates are x, y and z and the relative displacement components in these three directions are indicated with u, v and w, respectively. The base of this reference system is an orthonormal base indicated with the vectors, $\vec{e}_1$, $\vec{e}_2$ and $\vec{e}_3$.
- The orthogonal curvilinear system for the natural coordinates is indicated with (ξ, η, ζ), the base of this system is given by the three tangent vectors to the three coordinates, these vectors are $\vec{a}_\xi$, $\vec{a}_\eta$ and $\vec{a}_\zeta$, respectively.
- In each node is possible to consider a local tern of orthonormal vectors indicated with $\vec{a}_1$, $\vec{a}_2$ and $\vec{a}_3$. In this case the three coordinates for each node k are indicated as x^k, y^k and z^k.

Table 1
One-layered isotropic thin plate ($a/h = 1000$) with simply supported edges and transverse concentrated load P_z. Maximum transverse displacement w_{max} in 10^{-3} m.

	Ref. (Batoz and Dhatt, 1992)	9P-8N(iso)	9P-8N	RM	K
	4.64				
2×2		0.0034	4.63	4.63	4.63
4×4		0.4298	4.63	4.63	4.63
8×8		3.93	4.64	4.64	4.64
16×16		4.54	4.64	4.64	4.64
32×32		4.62	4.64	4.64	4.64

Table 2
One-layered isotropic thin plate ($a/h = 1000$) with clamped edges and transverse concentrated load P_z. Maximum transverse displacement w_{max} in 10^{-3} m.

	Ref. (Batoz and Dhatt, 1992)	9P-8N(iso)	9P-8N	RM	K
	2.24				
2×2		0.0002	2.18	2.20	2.20
4×4		0.0072	2.18	2.24	2.24
8×8		0.7602	2.22	2.24	2.24
16×16		2.10	2.23	2.24	2.24
32×32		2.21	2.24	2.24	2.24

- For a generic point in the middle surface, a local cartesian reference system can be indicated: the three coordinates are x', y' and z' and the relative displacement components are u', v' and w', respectively. The orthonormal base of this reference system is given by the vectors $\vec{e}'_1$, $\vec{e}'_2$ and $\vec{e}'_3$.

3. Refined kinematic shell model

The 9P-8N is a 9 parameter shell model because for each node of the 8-nodes shell element 9 degrees of freedom are considered. This means that for each displacement component a quadratic expansion in the thickness direction is assumed: this feature permits to have a linear transverse normal strain in the thickness direction which permits to avoid the Poisson locking phenomenon (Carrera and Brischetto, 2008a,b).

The three displacement components u, v and w in the global reference system are expressed as the three mid-surface displacements u_1, u_2 and u_3 in x, y and z direction, respectively, plus the linear $(\varphi'_1, \varphi'_2, \varphi'_3)$ and quadratic terms $(\psi'_1, \psi'_2, \psi'_3)$ given in the local reference system (x', y', z'). These local linear and quadratic terms are carried over the global reference system (the same used for the three mid-surface displacements) using the transformation matrix $[\Theta]$. The considered kinematic model is:

$$u = \begin{bmatrix} u \\ v \\ w \end{bmatrix} = \begin{bmatrix} u_1 \\ u_2 \\ u_3 \end{bmatrix} + [\Theta] z' \begin{bmatrix} \varphi'_1 \\ \varphi'_2 \\ \varphi'_3 \end{bmatrix} + [\Theta] z'^2 \begin{bmatrix} \psi'_1 \\ \psi'_2 \\ \psi'_3 \end{bmatrix}. \tag{1}$$

The transformation matrix $[\Theta]$ from local reference system (x', y', z') to global reference one (x, y, z) contains the scalar products between the local base vectors $(\vec{e}'_1, \vec{e}'_2, \vec{e}'_3)$ and the global base vectors $(\vec{e}_1, \vec{e}_2, \vec{e}_3)$:

$$[\Theta] = \begin{bmatrix} \vec{e}'_1 \cdot \vec{e}_1 & \vec{e}'_2 \cdot \vec{e}_1 & \vec{e}'_3 \cdot \vec{e}_1 \\ \vec{e}'_1 \cdot \vec{e}_2 & \vec{e}'_2 \cdot \vec{e}_2 & \vec{e}'_3 \cdot \vec{e}_2 \\ \vec{e}'_1 \cdot \vec{e}_3 & \vec{e}'_2 \cdot \vec{e}_3 & \vec{e}'_3 \cdot \vec{e}_3 \end{bmatrix} = \begin{bmatrix} t_{11} & t_{21} & t_{31} \\ t_{12} & t_{22} & t_{32} \\ t_{13} & t_{23} & t_{33} \end{bmatrix}. \tag{2}$$

The first step for a finite element (FE) approximation is the introduction of the shape functions $N_k(\xi, \eta)$ in order to express the global displacements as functions of the degrees of freedom in each node k (Zienkiewicz and Taylor, 2005; Batoz and Dhatt, 1992). An eight-nodes element (Q8), as indicated in Fig. 2, is considered where the shape functions $N_k(\xi, \eta)$ (with nodes k from 1 to 8) are:

$$\begin{aligned} N_1 &= \frac{-(1-\xi)(1-\eta)(1+\xi+\eta)}{4}, & N_2 &= \frac{-(1+\xi)(1-\eta)(1-\xi+\eta)}{4}, \\ N_3 &= \frac{-(1+\xi)(1+\eta)(1-\xi-\eta)}{4}, & N_4 &= \frac{-(1-\xi)(1+\eta)(1+\xi-\eta)}{4}, \\ N_5 &= \frac{\left(1-\xi^2\right)(1-\eta)}{2}, & N_6 &= \frac{(1-\eta^2)(1+\xi)}{2}, \\ N_7 &= \frac{\left(1-\xi^2\right)(1+\eta)}{2}, & N_8 &= \frac{(1-\eta^2)(1-\xi)}{2}. \end{aligned} \tag{3}$$

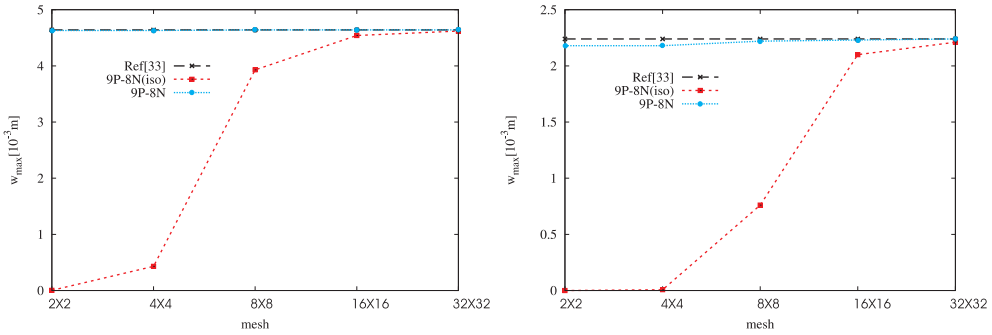

Fig. 5. One-layered isotropic thin plate ($a/h = 1000$) with simply supported edges (left) and clamped edges (right) subjected to transverse concentrated load P_z. Maximum transverse displacement w_{max} vs. mesh.

The introduction of shape functions $N_k(\xi, \eta)$ is possible if the natural coordinate ζ is coincident with the local one z'. After the FE approximation, the kinematic model is:

$$u = \begin{bmatrix} u(\xi,\eta,\zeta) \\ v(\xi,\eta,\zeta) \\ w(\xi,\eta,\zeta) \end{bmatrix} = N_k(\xi,\eta) \begin{bmatrix} u_{1k} \\ u_{2k} \\ u_{3k} \end{bmatrix} + \zeta[\Theta] N_k(\xi,\eta) \begin{bmatrix} \varphi'_{1k} \\ \varphi'_{2k} \\ \varphi'_{3k} \end{bmatrix} + \zeta^2[\Theta] N_k(\xi,\eta) \begin{bmatrix} \psi'_{1k} \\ \psi'_{2k} \\ \psi'_{3k} \end{bmatrix} \tag{4}$$

where the subscript k indicates the nodal degrees of freedom. In this way the derivatives of the three global displacement components are:

$$u_{,\xi} = \begin{bmatrix} u_{,\xi}(\xi,\eta,\zeta) \\ v_{,\xi}(\xi,\eta,\zeta) \\ w_{,\xi}(\xi,\eta,\zeta) \end{bmatrix} = N_{k,\xi}(\xi,\eta) \begin{bmatrix} u_{1k} \\ u_{2k} \\ u_{3k} \end{bmatrix} + \zeta[\Theta] N_{k,\xi}(\xi,\eta) \begin{bmatrix} \varphi'_{1k} \\ \varphi'_{2k} \\ \varphi'_{3k} \end{bmatrix} + \zeta^2[\Theta] N_{k,\xi}(\xi,\eta) \begin{bmatrix} \psi'_{1k} \\ \psi'_{2k} \\ \psi'_{3k} \end{bmatrix} \tag{5}$$

$$u_{,\eta} = \begin{bmatrix} u_{,\eta}(\xi,\eta,\zeta) \\ v_{,\eta}(\xi,\eta,\zeta) \\ w_{,\eta}(\xi,\eta,\zeta) \end{bmatrix} = N_{k,\eta}(\xi,\eta) \begin{bmatrix} u_{1k} \\ u_{2k} \\ u_{3k} \end{bmatrix} + \zeta[\Theta] N_{k,\eta}(\xi,\eta) \begin{bmatrix} \varphi'_{1k} \\ \varphi'_{2k} \\ \varphi'_{3k} \end{bmatrix} + \zeta^2[\Theta] N_{k,\eta}(\xi,\eta) \begin{bmatrix} \psi'_{1k} \\ \psi'_{2k} \\ \psi'_{3k} \end{bmatrix} \tag{6}$$

$$u_{,\zeta} = \begin{bmatrix} u_{,\zeta}(\xi,\eta,\zeta) \\ v_{,\zeta}(\xi,\eta,\zeta) \\ w_{,\zeta}(\xi,\eta,\zeta) \end{bmatrix} = [\Theta] N_k(\xi,\eta) \begin{bmatrix} \varphi'_{1k} \\ \varphi'_{2k} \\ \varphi'_{3k} \end{bmatrix} + 2\zeta[\Theta] N_k(\xi,\eta) \begin{bmatrix} \psi'_{1k} \\ \psi'_{2k} \\ \psi'_{3k} \end{bmatrix} \tag{7}$$

4. Local strains for the refined shell model

In order to simplify the interpolation of the shell assumption, the strain components should be defined in terms of the local system axes (where z' is perpendicular to the $\xi\eta$-plane). The local system of axes is also the most convenient system for expressing the stress components (and their resultants) for shell analysis and design (Huang and Hinton, 1986). The local strains, split in in-plane ($\varepsilon'_p = [\varepsilon'_{x'x'}, \varepsilon'_{y'y'}, \gamma'_{x'y'}]^T$) and out-of-plane components ($\varepsilon'_n = [\gamma'_{y'z'} \gamma'_{x',z'} \varepsilon'_{z'z'}]^T$), are:

$$\varepsilon' = \begin{bmatrix} \varepsilon'_p \\ \varepsilon'_n \end{bmatrix} = \begin{bmatrix} \varepsilon'_{x'x'} \\ \varepsilon'_{y'y'} \\ \gamma'_{x'y'} \\ \gamma'_{y'z'} \\ \gamma'_{x'z'} \\ \varepsilon'_{z'z'} \end{bmatrix} = \begin{bmatrix} u'_{x'} \\ v'_{y'} \\ u'_{y'} + v'_{x'} \\ v'_{z'} + w'_{y'} \\ u'_{z'} + w'_{x'} \\ w'_{z'} \end{bmatrix}. \tag{8}$$

The subscripts, containing the three local coordinates, indicate the partial derivatives. In order to obtain the relations in Eq. (8), it is necessary to calculate the local displacements derived with respect to local coordinates. The first step is to obtain the global displacements derived with respect to global coordinates using the global displacements derived with respect to natural coordinates (see Eqs. (5)–(7)):

$$\begin{bmatrix} u_{,x} & v_{,x} & w_{,x} \\ u_{,y} & v_{,y} & w_{,y} \\ u_{,z} & v_{,z} & w_{,z} \end{bmatrix} = \begin{bmatrix} J^*_{11} & J^*_{12} & J^*_{13} \\ J^*_{21} & J^*_{22} & J^*_{23} \\ J^*_{31} & J^*_{32} & J^*_{33} \end{bmatrix} \begin{bmatrix} u_{,\xi} & v_{,\xi} & w_{,\xi} \\ u_{,\eta} & v_{,\eta} & w_{,\eta} \\ u_{,\zeta} & v_{,\zeta} & w_{,\zeta} \end{bmatrix}, \tag{9}$$

where the (3×3) Jacobian matrix $[J]$ and its inverse $[J]^{-1}$ are:

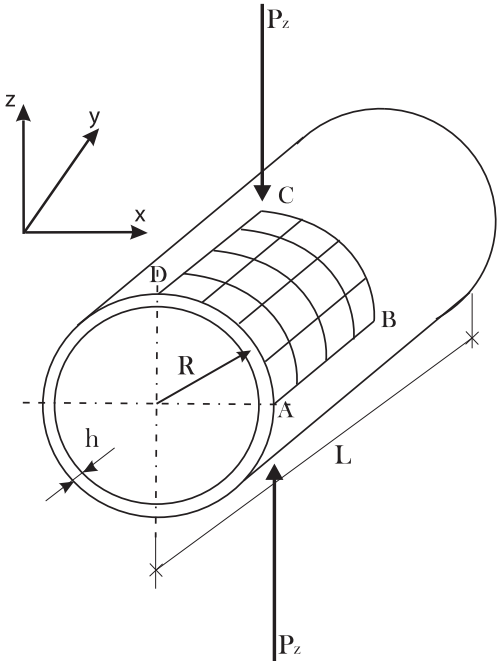

Fig. 6. Pinched cylindrical shell. One-layered and multilayered isotropic/composite configurations.

Table 3
One-layered isotropic pinched cylindrical shell ($R/h = 100$). Maximum transverse displacement w_{max} in 10^{-6} m at the point C.

	Flügge 1973	Reddy 2004	Zhao et al. 2008	9P-8N(iso)	9P-8N(SL)	9P-8N	RM	K
	−0.18248	−0.18661	−0.18663					
2 × 2				−0.00785	−0.06124	−0.08366	−0.08755	−0.08695
4 × 4				−0.02649	−0.14659	−0.15932	−0.16093	−0.16011
8 × 8				−0.09337	−0.15266	−0.18139	−0.18181	−0.18044
16 × 16				−0.16209	−0.18073	−0.18600	−0.18588	−0.18315
32 × 32				−0.18085	−0.18441	−0.18680	−0.18620	−0.18330

$$[J] = \begin{bmatrix} \frac{\partial x}{\partial \xi} & \frac{\partial y}{\partial \xi} & \frac{\partial z}{\partial \xi} \\ \frac{\partial x}{\partial \eta} & \frac{\partial y}{\partial \eta} & \frac{\partial z}{\partial \eta} \\ \frac{\partial x}{\partial \zeta} & \frac{\partial y}{\partial \zeta} & \frac{\partial z}{\partial \zeta} \end{bmatrix}, \quad [J]^{-1} = \begin{bmatrix} J^*_{11} & J^*_{12} & J^*_{13} \\ J^*_{21} & J^*_{22} & J^*_{23} \\ J^*_{31} & J^*_{32} & J^*_{33} \end{bmatrix}. \tag{10}$$

Finally, in order to obtain the local displacements derived with respect to local coordinates (x', y', z') for the strain relations in Eq. (8), the matrix $[\Theta]$ of scalar products of Eq. (2) is used:

$$\begin{bmatrix} u'_{,x'} & v'_{,x'} & w'_{,x'} \\ u'_{,y'} & v'_{,y'} & w'_{,y'} \\ u'_{,z'} & v'_{,z'} & w'_{,z'} \end{bmatrix} = [\Theta] \begin{bmatrix} u_{,x} & v_{,x} & w_{,x} \\ u_{,y} & v_{,y} & w_{,y} \\ u_{,z} & v_{,z} & w_{,z} \end{bmatrix} [\Theta]^T. \tag{11}$$

The explicit forms of the six local strain components, written in a compact matrix form, are:

$$\begin{aligned} \varepsilon'_p &= \left[F_\zeta\right][\mathrm{Geo}_p][\mathrm{BDOF}], \\ \varepsilon'_n &= \left[F_\zeta\right][\mathrm{Geo}_n][\mathrm{BDOF}], \end{aligned} \tag{12}$$

in Eq. (12) the matrix $[F_\zeta]$ has dimension (3×9) and contains the thickness parameters:

$$\left[F_\zeta\right] = \begin{bmatrix} 1 & \zeta & \zeta^2 & 0 & 0 & 0 & 0 & 0 & 0 \\ 0 & 0 & 0 & 1 & \zeta & \zeta^2 & 0 & 0 & 0 \\ 0 & 0 & 0 & 0 & 0 & 0 & 1 & \zeta & \zeta^2 \end{bmatrix}, \tag{13}$$

the vector [BDOF] has dimension (27×1), and it contains the degrees of freedom and their derivatives for each node k:

$$\begin{aligned} [\mathrm{BDOF}]^T = \big[[Nu][N\varphi'][N\psi']\big] = \big[& N_k u_{1k} N_{k,\xi} u_{1k} N_{k,\eta} u_{1k} N_k u_{2k} \\ & N_{k,\xi} u_{2k} N_{k,\eta} u_{2k} N_k u_{3k} N_{k,\xi} u_{3k} N_{k,\eta} u_{3k} N_k \varphi'_{1k} N_{k,\xi} \varphi'_{1k} \\ & N_{k,\eta} \varphi'_{1k} N_k \varphi'_{2k} N_{k,\xi} \varphi'_{2k} N_{k,\eta} \varphi'_{2k} N_k \varphi'_{3k} N_{k,\xi} \varphi'_{3k} N_{k,\eta} \varphi'_{3k} \\ & N_k \psi'_{1k} N_{k,\xi} \psi'_{1k} N_{k,\eta} \psi'_{1k} N_k \psi'_{2k} N_{k,\xi} \psi'_{2k} N_{k,\eta} \psi'_{2k} N_k \psi'_{3k} \\ & N_{k,\xi} \psi'_{3k} N_{k,\eta} \psi'_{3k} \big] \end{aligned} \tag{14}$$

The two matrices $[\mathrm{Geo}_p]$ and $[\mathrm{Geo}_n]$ contain the geometrical parameters for the in-plane (p) and out-plane (n) strain components, they have dimension (9×27), each matrix can be split in three submatrices of dimension (9×9):

$$[\mathrm{Geo}_p] = \left[[G_{\mathrm{up}}][G_{\varphi' p}]\left[G_{\psi' p}\right]\right], \tag{15}$$

$$[\mathrm{Geo}_n] = \left[[G_{\mathrm{un}}][G_{\varphi' n}]\left[G_{\psi' n}\right]\right], \tag{16}$$

where

$$[G_{\mathrm{up}}] = \begin{bmatrix} 0 & A_1 & B_1 & 0 & C_1 & D_1 & 0 & E_1 & F_1 \\ 0 & 0 & 0 & 0 & 0 & 0 & 0 & 0 & 0 \\ 0 & 0 & 0 & 0 & 0 & 0 & 0 & 0 & 0 \\ 0 & A_2 & B_2 & 0 & C_2 & D_2 & 0 & E_2 & F_2 \\ 0 & 0 & 0 & 0 & 0 & 0 & 0 & 0 & 0 \\ 0 & 0 & 0 & 0 & 0 & 0 & 0 & 0 & 0 \\ 0 & A_3 & B_3 & 0 & C_3 & D_3 & 0 & E_3 & F_3 \\ 0 & 0 & 0 & 0 & 0 & 0 & 0 & 0 & 0 \\ 0 & 0 & 0 & 0 & 0 & 0 & 0 & 0 & 0 \end{bmatrix}, \tag{17}$$

$$[G_{\varphi' p}] = \begin{bmatrix} G'_1 & 0 & 0 & H'_1 & 0 & 0 & I'_1 & 0 & 0 \\ 0 & A'_1 & B'_1 & 0 & C'_1 & D'_1 & 0 & E'_1 & F'_1 \\ 0 & 0 & 0 & 0 & 0 & 0 & 0 & 0 & 0 \\ G'_2 & 0 & 0 & H'_2 & 0 & 0 & I'_2 & 0 & 0 \\ 0 & A'_2 & B'_2 & 0 & C'_2 & D'_2 & 0 & E'_2 & F'_2 \\ 0 & 0 & 0 & 0 & 0 & 0 & 0 & 0 & 0 \\ G'_3 & 0 & 0 & H'_3 & 0 & 0 & I'_3 & 0 & 0 \\ 0 & A'_3 & B'_3 & 0 & C'_3 & D'_3 & 0 & E'_3 & F'_3 \\ 0 & 0 & 0 & 0 & 0 & 0 & 0 & 0 & 0 \end{bmatrix}, \tag{18}$$

$$\left[G_{\psi' p}\right] = \begin{bmatrix} 0 & 0 & 0 & 0 & 0 & 0 & 0 & 0 & 0 \\ 2G'_1 & 0 & 0 & 2H'_1 & 0 & 0 & 2I'_1 & 0 & 0 \\ 0 & A'_1 & B'_1 & 0 & C'_1 & D'_1 & 0 & E'_1 & F'_1 \\ 0 & 0 & 0 & 0 & 0 & 0 & 0 & 0 & 0 \\ 2G'_2 & 0 & 0 & 2H'_2 & 0 & 0 & 2I'_2 & 0 & 0 \\ 0 & A'_2 & B'_2 & 0 & C'_2 & D'_2 & 0 & E'_2 & F'_2 \\ 0 & 0 & 0 & 0 & 0 & 0 & 0 & 0 & 0 \\ 2G'_3 & 0 & 0 & 2H'_3 & 0 & 0 & 2I'_3 & 0 & 0 \\ 0 & A'_3 & B'_3 & 0 & C'_3 & D'_3 & 0 & E'_3 & F'_3 \end{bmatrix}, \tag{19}$$

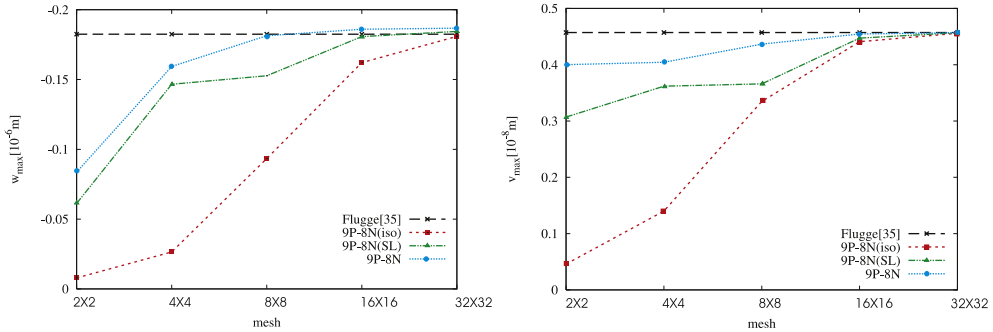

Fig. 7. One-layered isotropic pinched cylindrical shell ($R/h = 100$). Maximum transverse displacement w_{max} vs. mesh (left) and maximum longitudinal displacement v_{max} vs. mesh (right).

Table 4
One-layered isotropic pinched cylindrical shell ($R/h = 100$). Maximum longitudinal displacement v_{max} in 10^{-8} m at the point D.

	Flügge 1973	9P-8N(iso)	9P-8N(SL)	9P-8N	RM	K
	0.45711					
2×2		0.04590	0.30703	0.40016	0.40007	0.40316
4×4		0.14016	0.36194	0.40444	0.40758	0.40678
8×8		0.33477	0.36599	0.43671	0.43723	0.43569
16×16		0.44086	0.44725	0.45465	0.45466	0.44032
32×32		0.45578	0.45673	0.45683	0.45681	0.45664

$$[G_{un}] = \begin{bmatrix} 0 & A_4 & B_4 & 0 & C_4 & D_4 & 0 & E_4 & F_4 \\ 0 & 0 & 0 & 0 & 0 & 0 & 0 & 0 & 0 \\ 0 & 0 & 0 & 0 & 0 & 0 & 0 & 0 & 0 \\ 0 & A_5 & B_5 & 0 & C_5 & D_5 & 0 & E_5 & F_5 \\ 0 & 0 & 0 & 0 & 0 & 0 & 0 & 0 & 0 \\ 0 & 0 & 0 & 0 & 0 & 0 & 0 & 0 & 0 \\ 0 & A_6 & B_6 & 0 & C_6 & D_6 & 0 & E_6 & F_6 \\ 0 & 0 & 0 & 0 & 0 & 0 & 0 & 0 & 0 \\ 0 & 0 & 0 & 0 & 0 & 0 & 0 & 0 & 0 \end{bmatrix}, \tag{20}$$

$$[G_{\varphi' n}] = \begin{bmatrix} G'_4 & 0 & 0 & H'_4 & 0 & 0 & I'_4 & 0 & 0 \\ 0 & A'_4 & B'_4 & 0 & C'_4 & D'_4 & 0 & E'_4 & F'_4 \\ 0 & 0 & 0 & 0 & 0 & 0 & 0 & 0 & 0 \\ G'_5 & 0 & 0 & H'_5 & 0 & 0 & I'_5 & 0 & 0 \\ 0 & A'_5 & B'_5 & 0 & C'_5 & D'_5 & 0 & E'_5 & F'_5 \\ 0 & 0 & 0 & 0 & 0 & 0 & 0 & 0 & 0 \\ G'_6 & 0 & 0 & H'_6 & 0 & 0 & I'_6 & 0 & 0 \\ 0 & A'_6 & B'_6 & 0 & C'_6 & D'_6 & 0 & E'_6 & F'_6 \\ 0 & 0 & 0 & 0 & 0 & 0 & 0 & 0 & 0 \end{bmatrix}, \tag{21}$$

$$[G_{\psi' n}] = \begin{bmatrix} 0 & 0 & 0 & 0 & 0 & 0 & 0 & 0 & 0 \\ 2G'_4 & 0 & 0 & 2H'_4 & 0 & 0 & 2I'_4 & 0 & 0 \\ 0 & A'_4 & B'_4 & 0 & C'_4 & D'_4 & 0 & E'_4 & F'_4 \\ 0 & 0 & 0 & 0 & 0 & 0 & 0 & 0 & 0 \\ 2G'_5 & 0 & 0 & 2H'_5 & 0 & 0 & 2I'_5 & 0 & 0 \\ 0 & A'_5 & B'_5 & 0 & C'_5 & D'_5 & 0 & E'_5 & F'_5 \\ 0 & 0 & 0 & 0 & 0 & 0 & 0 & 0 & 0 \\ 2G'_6 & 0 & 0 & 2H'_6 & 0 & 0 & 2I'_6 & 0 & 0 \\ 0 & A'_6 & B'_6 & 0 & C'_6 & D'_6 & 0 & E'_6 & F'_6 \end{bmatrix}. \tag{22}$$

The meaning of the geometric coefficients used in matrices of Eqs. (17)–(22) are given in explicit form in the Appendix A, they contain all the information about the geometry of the shell (the scalar products components and the Jacobian components).

$$[\mathrm{DOF}]^T = \left[[\mathrm{DOF}u]^T \; [\mathrm{DOF}\varphi']^T \; [\mathrm{DOF}\psi']^T \right] = \left[\{u_1\}_{k=1,8} \; \{u_2\}_{k=1,8} \; \{u_3\}_{k=1,8} \; \{\varphi'_1\}_{k=1,8} \; \{\varphi'_2\}_{k=1,8} \; \{\varphi'_3\}_{k=1,8} \; \{\psi'_1\}_{k=1,8} \; \{\psi'_2\}_{k=1,8} \; \{\psi'_3\}_{k=1,8} \right]. \tag{24}$$

The matrix of shape functions and their derivatives [B] of dimension (27×72), has three blocks of dimension (9×24) along its diagonal, these three blocks are the same and they are indicated with $[Bf] = [Bu] = [B\varphi'] = [B\psi']$:

$$[B] = \begin{bmatrix} [Bu] & [0] & [0] \\ [0] & [B\varphi'] & [0] \\ [0] & [0] & [B\psi'] \end{bmatrix}, \tag{25}$$

the explicit form of each block is:

$$[Bf] = \begin{bmatrix} [N] & [0] & [0] \\ [0] & [N] & [0] \\ [0] & [0] & [N] \end{bmatrix}, \tag{26}$$

where the matrix [N] contains the shape functions and their derivatives for each node ($k = 1,8$):

$$[N] = \begin{bmatrix} N_1 & N_2 & N_3 & N_4 & N_5 & N_6 & N_7 & N_8 \\ N_{1,\xi} & N_{2,\xi} & N_{3,\xi} & N_{4,\xi} & N_{5,\xi} & N_{6,\xi} & N_{7,\xi} & N_{8,\xi} \\ N_{1,\eta} & N_{2,\eta} & N_{3,\eta} & N_{4,\eta} & N_{5,\eta} & N_{6,\eta} & N_{7,\eta} & N_{8,\eta} \end{bmatrix}. \tag{27}$$

By using Eqs. (23) and (24), the Eq. (12) can be written as:

$$\begin{aligned} \varepsilon'_p &= \left[F_\zeta\right] [\mathrm{Geo}_p] [B] [\mathrm{DOF}], \\ \varepsilon'_n &= \left[F_\zeta\right] [\mathrm{Geo}_n] [B] [\mathrm{DOF}]. \end{aligned} \tag{28}$$

By using the Eqs. (15), (16), (24) and (25), the Eq. (28) is written in the following way:

$$\begin{aligned} \varepsilon'_p &= \left[F_\zeta\right] \left([G_{\mathrm{up}}] [Bu] [\mathrm{DOF}_u] + [G_{\varphi' p}] [B\varphi'] [\mathrm{DOF}\varphi'] + \left[G_{\psi' p}\right] [B\psi'] [\mathrm{DOF}\psi'] \right), \\ \varepsilon'_n &= \left[F_\zeta\right] \left([G_{\mathrm{un}}] [Bu] [\mathrm{DOF}_u] + [G_{\varphi' \mathrm{n}}] [B\varphi'] [\mathrm{DOF}\varphi'] + \left[G_{\psi' \mathrm{n}}\right] [B\psi'] [\mathrm{DOF}\psi'] \right). \end{aligned} \tag{29}$$

The vector [BDOF] of dimension (27×1) indicated in Eq. (14) can be written in matrix form split in the matrix [B] containing the shape functions and their derivatives (dimension (27×72)) and the array containing the degrees of freedom [DOF] (dimension (72×1)):

$$[\mathrm{BDOF}] = [B][\mathrm{DOF}]. \tag{23}$$

The vector containing the degrees of freedom is split in three sub-arrays [DOFu], [DOFφ'] and [DOFψ'], each one of dimension (24×1):

These are the geometrical relations, written in matrix form, which are used in the variational statement in order to obtain the global stiffness matrix for the proposed finite element shell.

5. Constitutive equations for isotropic and orthotropic composite structures

The 9P-8N model considers a quadratic expansion in the thickness direction z for the transverse displacement w, therefore the transverse normal strain $\varepsilon'_{z'z'}$ is linear in the thickness direction: as discussed in Carrera and Brischetto (2008a,b) this feature permits

Table 5
One-layered isotropic moderately thin and thick plates with simply supported edges and transverse concentrated load P_z. Maximum transverse displacement w_{max} in 10^{-6} m and 10^{-9} m for $a/h = 100$ and $a/h = 10$, respectively.

	9P-8N	RM($\chi = 5/6$)	RM	K
$a/h = 100$				
2×2	4.63	4.64	4.63	4.63
4×4	4.63	4.64	4.63	4.63
8×8	4.65	4.65	4.65	4.64
16×16	4.66	4.66	4.66	4.64
32×32	4.67	4.67	4.67	4.64
$a/h = 10$				
2×2	5.17	5.21	5.12	4.63
4×4	5.44	5.51	5.37	4.63
8×8	5.65	5.69	5.53	4.64
16×16	5.87	5.83	5.66	4.64
32×32	6.13	5.96	5.77	4.64

to obtain an element free of Poisson thickness locking, and 3D constitutive equations can be used as proposed in Reddy 2004. Constitutive equations give a relation between stress components and strain ones. The local stress components vector of dimension (6×1) is in relation with the local strain components vector of dimension (6×1) via the matrix $[Q]$ of dimension $[6 \times 6]$ containing the elastic coefficients. In general the relation is:

$$\boldsymbol{\sigma}' = [Q]\boldsymbol{\varepsilon}'. \tag{30}$$

The vectors of stress and strain components are:

$$\boldsymbol{\sigma}' = \left[\sigma'_{x'x'}\ \sigma'_{y'y'}\ \sigma'_{z'z'}\ \sigma'_{y'z'}\ \sigma'_{x'z'}\ \sigma'_{x'y'}\right]^T, \tag{31}$$

$$\boldsymbol{\varepsilon}' = \left[\varepsilon'_{x'x'}\ \varepsilon'_{y'y'}\ \varepsilon'_{z'z'}\ \gamma'_{y'z'}\ \gamma'_{x'z'}\ \gamma'_{x'y'}\right]^T, \tag{32}$$

The matrix of elastic coefficients $[Q]$ is obtained in the structural reference system of an orthotropic composite structure, these coefficients are linked with the elastic coefficients matrix $[C]$ written in the material reference system by the well-known relations given in Reddy 2004 (structural and material reference systems are the systems employed to analyze the behavior of composite orthotropic materials and they do not concern the finite element shell approximation):

$$[Q] = \begin{bmatrix} Q_{11} & Q_{12} & Q_{13} & 0 & 0 & Q_{16} \\ Q_{12} & Q_{22} & Q_{23} & 0 & 0 & Q_{26} \\ Q_{13} & Q_{23} & Q_{33} & 0 & 0 & Q_{36} \\ 0 & 0 & 0 & Q_{44} & Q_{45} & 0 \\ 0 & 0 & 0 & Q_{45} & Q_{55} & 0 \\ Q_{16} & Q_{26} & Q_{36} & 0 & 0 & Q_{66} \end{bmatrix}. \tag{33}$$

Table 6
One-layered isotropic moderately thin and thick plates with clamped edges and transverse concentrated load P_z. Maximum transverse displacement w_{max} in 10^{-6} m and 10^{-9} m for $a/h = 100$ and $a/h = 10$, respectively.

	9P-8N	RM ($\chi = 5/6$)	RM	K
$a/h = 100$				
2×2	2.15	2.20	2.20	2.19
4×4	2.19	2.24	2.24	2.24
8×8	2.22	2.25	2.25	2.24
16×16	2.24	2.25	2.25	2.24
32×32	2.25	2.25	2.25	2.24
$a/h = 10$				
2×2	2.80	2.90	2.80	2.19
4×4	2.81	2.92	2.81	2.24
8×8	3.00	3.05	2.92	2.24
16×16	3.21	3.18	3.02	2.24
32×32	3.46	3.30	3.13	2.24

Table 7
One-layered orthotropic thin plate ($a/h = 1000$) with simply supported edges and transverse concentrated load P_z. Maximum transverse no-dimensional displacement $\overline{w}$.

	Ref. (Bhaskar and Kaushik, 2004)	9P-8N	RM	K
	0.02324			
2×2		0.02303	0.02303	0.02303
4×4		0.02308	0.02308	0.02308
8×8		0.02320	0.02320	0.02320
16×16		0.02323	0.02323	0.02323
32×32		0.02324	0.02324	0.02324

In order to use the constitutive equations in the Principle of Virtual Displacements, it is very useful to split the stress and strain components in in-plane (p) and out-of-plane (n) contributes:

$$\begin{bmatrix} \sigma'_{x'x'} \\ \sigma'_{y'y'} \\ \sigma'_{x'y'} \\ \sigma'_{y'z'} \\ \sigma'_{x'z'} \\ \sigma'_{z'z'} \end{bmatrix} = \begin{bmatrix} Q_{11} & Q_{12} & Q_{16} & 0 & 0 & Q_{13} \\ Q_{12} & Q_{22} & Q_{26} & 0 & 0 & Q_{23} \\ Q_{16} & Q_{26} & Q_{66} & 0 & 0 & Q_{36} \\ 0 & 0 & 0 & Q_{44} & Q_{45} & 0 \\ 0 & 0 & 0 & Q_{45} & Q_{55} & 0 \\ Q_{13} & Q_{23} & Q_{36} & 0 & 0 & Q_{33} \end{bmatrix} \begin{bmatrix} \varepsilon'_{x'x'} \\ \varepsilon'_{y'y'} \\ \gamma'_{x'y'} \\ \gamma'_{y'z'} \\ \gamma'_{x'z'} \\ \varepsilon'_{z'z'} \end{bmatrix}. \tag{34}$$

The vectors of in-plane and out-of-plane strain and stress components are:

$$\begin{aligned} \sigma'_p &= \left[\sigma'_{x'x'}\ \sigma'_{y'y'}\ \sigma'_{x'y'}\right]^T, \quad \sigma'_n = \left[\sigma'_{y'z'}\ \sigma'_{x'z'}\ \sigma'_{z'z'}\right]^T, \\ \varepsilon'_p &= \left[\varepsilon'_{x'x'}\ \varepsilon'_{y'y'}\ \gamma'_{x'y'}\right]^T, \quad \varepsilon'_n = \left[\gamma'_{y'z'}\ \gamma'_{x'z'}\ \varepsilon'_{z'z'}\right]^T. \end{aligned} \tag{35}$$

In this way the constitutive equations are split in the following form:

$$\sigma'_p = [Q_{pp}]\varepsilon'_p + [Q_{pn}]\varepsilon'_n, \tag{36}$$

$$\sigma'_n = [Q_{np}]\varepsilon'_p + [Q_{nn}]\varepsilon'_n, \tag{37}$$

where:

$$[Q_{pp}] = \begin{bmatrix} Q_{11} & Q_{12} & Q_{16} \\ Q_{12} & Q_{22} & Q_{26} \\ Q_{16} & Q_{26} & Q_{66} \end{bmatrix}, \quad [Q_{pn}] = \begin{bmatrix} 0 & 0 & Q_{13} \\ 0 & 0 & Q_{23} \\ 0 & 0 & Q_{36} \end{bmatrix}, \tag{38}$$

$$[Q_{np}] = \begin{bmatrix} 0 & 0 & 0 \\ 0 & 0 & 0 \\ Q_{13} & Q_{23} & Q_{36} \end{bmatrix}, \quad [Q_{nn}] = \begin{bmatrix} Q_{44} & Q_{45} & 0 \\ Q_{45} & Q_{55} & 0 \\ 0 & 0 & Q_{33} \end{bmatrix}. \tag{39}$$

6. Governing equations and global stiffness matrix

In order to obtain the global stiffness matrix $[K]$ (the dimension is 72×72) of the employed finite element shell 9P-8N, the Principle

Table 8
One-layered orthotropic thin plate ($a/h = 1000$) with clamped edges and transverse concentrated load P_z. Maximum transverse no-dimensional displacement $\overline{w}$.

	Ref. (Bhaskar and Kaushik, 2004)	9P-8N	RM	K
	0.009167			
2×2		0.006998	0.007013	0.007012
4×4		0.007815	0.007829	0.007820
8×8		0.009041	0.009045	0.009032
16×16		0.009152	0.009154	0.009148
32×32		0.009167	0.009167	0.009164

Table 9
Three-layered orthotropic (0°/90°/0°) thin plate ($a/h = 1000$) with simply supported edges and transverse concentrated load P_z. Maximum transverse no-dimensional displacement $\overline{w}$.

	Ref. (Bhaskar and Kaushik, 2004)	9P-8N	RM	K
	0.02131			
2×2		0.02100	0.02109	0.02109
4×4		0.02119	0.02119	0.02119
8×8		0.02128	0.02128	0.02128
16×16		0.02130	0.02130	0.02130
32×32		0.02131	0.02131	0.02130

of Virtual Displacements (PVD) is written for the considered multilayered structure:

$$\delta L_i = \int_V \delta\boldsymbol{\varepsilon}'^T \boldsymbol{\sigma}' \mathrm{d}V = \int_\Omega \int_A (\delta\boldsymbol{\varepsilon}'^T_{pG}\boldsymbol{\sigma}'_{pC} + \delta\boldsymbol{\varepsilon}'^T_{nG}\boldsymbol{\sigma}'_{nC})\mathrm{d}\Omega\,\mathrm{d}\zeta = \delta L_e, \tag{40}$$

where δL_i is the virtual variation of the internal work and δL_e the external one, V is the volume of the considered multilayered structure, Ω is the integration domain in the plane, A is the integration domain in the thickness direction, T means the transpose of a vector or matrix. Subscript G means substitution of geometrical relations of Section 4, subscript C means substitution of constitutive equations written in split form in Section 5. Bold letters before the substitution of geometrical and constitutive equations mean arrays or matrices, in this work the arrays and matrices are also indicated with the symbol [ ].

For a eight node shell element the system of governing equations is:

$$\delta[\mathrm{DOF}]: \quad [K][\mathrm{DOF}] = [P]. \tag{41}$$

In Eq. (41) the vector $[P]$ has dimension (72×1) and it contains the mechanical loads. The vector of degrees of freedom $[DOF]$ of dimension (72×1) is that in Eq. (24). The stiffness matrix of the shell element has dimension (72×72) and it is considered as a block of 9 matrices of dimension (24×24). The matrix $[K]$ is:

$$[K] = \begin{bmatrix} [K_{uu}] & [K_{u\varphi'}] & [K_{u\psi'}] \\ [K_{\varphi' u}] & [K_{\varphi'\varphi'}] & [K_{\varphi'\psi'}] \\ [K_{\psi' u}] & [K_{\psi'\varphi'}] & [K_{\psi'\psi'}] \end{bmatrix}. \tag{42}$$

The nine sub-arrays of the stiffness matrix $[K]$ have dimension (24×24), they are considered for the multilayered structures at the element level. The considered element is a shell element with eight nodes, the assembly procedure to obtain the stiffness matrix at multilayer level is the Equivalent Single Layer (ESL) approach.

The explicit forms of the nine sub-arrays are:

Table 10
Three-layered orthotropic (0°/90°/0°) thin plate ($a/h = 1000$) with clamped edges and transverse concentrated load P_z. Maximum transverse no-dimensional displacement $\overline{w}$.

	Ref. (Bhaskar and Kaushik, 2004)	9P-8N	RM	K
	0.008175			
2×2		0.006998	0.007013	0.007012
4×4		0.007463	0.007472	0.007466
8×8		0.008108	0.008111	0.008104
16×16		0.008166	0.008168	0.008164
32×32		0.008175	0.008176	0.008173

Table 11
One-layered orthotropic (90°) pinched cylindrical shell ($R/h = 100$). Maximum transverse no-dimensional displacement $\overline{w}$ at the point C.

	Flügge (Jones, 2002)	Sanders (Jones, 2002)	ABAQUS (Jones, 2002)	9P-8N	RM	K
	2819.8	2895.8	2885.5			
2×2				888.56	894.82	839.68
4×4				2532.7	2536.7	2508.0
8×8				2884.1	2886.0	2843.0
16×16				2886.3	2885.2	2842.5
32×32				2887.3	2885.3	2825.6

$$\begin{aligned}[K_{uu}] = \int_\Omega \Big\{ &[Bu]^T [G_{up}]^T [A_{pp}] [G_{up}] [Bu] \\ &+[Bu]^T [G_{up}]^T [A_{pn}] [G_{un}] [Bu] \\ &+[Bu]^T [G_{un}]^T [A_{np}] [G_{up}] [Bu] \\ &+[Bu]^T [G_{un}]^T [A_{nn}] [G_{un}] [Bu] \Big\} |\boldsymbol{J}| \mathrm{d}\xi \mathrm{d}\eta, \end{aligned} \tag{43}$$

$$\begin{aligned}[K_{u\varphi'}] = \int_\Omega \Big\{ &[Bu]^T [G_{up}]^T [A_{pp}] [G_{\varphi' p}] [B\varphi'] \\ &+ [Bu]^T [G_{up}]^T [A_{pn}] [G_{\varphi' n}] [B\varphi'] \\ &+ [Bu]^T [G_{un}]^T [A_{np}] [G_{\varphi' p}] [B\varphi'] \\ &+ [Bu]^T [G_{un}]^T [A_{nn}] [G_{\varphi' n}] [B\varphi'] \Big\} |\boldsymbol{J}| \mathrm{d}\xi \mathrm{d}\eta, \end{aligned} \tag{44}$$

$$\begin{aligned}\left[K_{u\psi'}\right] = \int_\Omega \Big\{ &[Bu]^T [G_{up}]^T [A_{pp}] \left[G_{\psi' p}\right] [B\psi'] \\ &+ [Bu]^T [G_{up}]^T [A_{pn}] \left[G_{\psi' n}\right] [B\psi'] \\ &+ [Bu]^T [G_{un}]^T [A_{np}] \left[G_{\psi' p}\right] [B\psi'] \\ &+ [Bu]^T [G_{un}]^T [A_{nn}] \left[G_{\psi' n}\right] [B\psi'] \Big\} |\boldsymbol{J}| \mathrm{d}\xi \mathrm{d}\eta, \end{aligned} \tag{45}$$

$$\begin{aligned}[K_{\varphi' u}] = \int_\Omega \Big\{ &[B\varphi']^T [G_{\varphi' p}]^T [A_{pp}] [G_{up}] [Bu] \\ &+ [B\varphi']^T [G_{\varphi' p}]^T [A_{pn}] [G_{un}] [Bu] \\ &+ [B\varphi']^T [G_{\varphi' n}]^T [A_{np}] [G_{up}] [Bu] \\ &+ [B\varphi']^T [G_{\varphi' n}]^T [A_{nn}] [G_{un}] [Bu] \Big\} |\boldsymbol{J}| \mathrm{d}\xi \mathrm{d}\eta, \end{aligned} \tag{46}$$

$$\begin{aligned}[K_{\varphi'\varphi'}] = \int_\Omega \Big\{ &[B\varphi']^T [G_{\varphi' p}]^T [A_{pp}] [G_{\varphi' p}] [B\varphi'] \\ &+ [B\varphi']^T [G_{\varphi' p}]^T [A_{pn}] [G_{\varphi' n}] [B\varphi'] \\ &+ [B\varphi']^T [G_{\varphi' n}]^T [A_{np}] [G_{\varphi' p}] [B\varphi'] \\ &+ [B\varphi']^T [G_{\varphi' n}]^T [A_{nn}] [G_{\varphi' n}] [B\varphi'] \Big\} |\boldsymbol{J}| \mathrm{d}\xi \mathrm{d}\eta, \end{aligned} \tag{47}$$

Table 12
One-layered orthotropic (0°) pinched cylindrical shell ($R/h = 100$). Maximum transverse no-dimensional displacement $\overline{w}$ at the point C.

	Flügge (Jones, 2002)	Sanders (Jones, 2002)	ABAQUS (Jones, 2002)	9P-8N	RM	K
	932.98	1005.0	991.21			
2×2				685.90	689.20	675.70
4×4				834.08	834.67	802.60
8×8				974.30	974.45	938.75
16×16				1019.7	1019.0	966.28
32×32				1026.6	1024.9	970.87

Table 13
Three-layered orthotropic (90°/0°/90°) pinched cylindrical shell ($R/h = 100$). Maximum transverse no-dimensional displacement $\overline{w}$ at the point C.

	Flügge (Jones, 2002)	Sanders (Jones, 2002)	ABAQUS (Jones, 2002)	9P-8N	RM	K
	1843.3	1913.5	1914.7			
2×2				702.23	702.61	645.77
4×4				1657.3	1658.4	1628.9
8×8				1768.7	1768.7	1729.8
16×16				1897.3	1896.6	1843.6
32×32				1900.0	1898.4	1846.0

$$\begin{aligned}\left[K_{\varphi'\psi'}\right] = \int_\Omega \Big\{ & [B\varphi']^T [G_{\varphi' p}]^T [A_{\mathrm{pp}}] \left[G_{\psi' p}\right] [B\psi'] \\ & + [B\varphi']^T [G_{\varphi' p}]^T [A_{\mathrm{pn}}] \left[G_{\psi' n}\right] [B\psi'] \\ & + [B\varphi']^T [G_{\varphi' n}]^T [A_{\mathrm{np}}] \left[G_{\psi' p}\right] [B\psi'] \\ & + [B\varphi']^T [G_{\varphi' n}]^T [A_{\mathrm{nn}}] \left[G_{\psi' n}\right] [B\psi'] \Big\} |\boldsymbol{J}| d\xi d\eta, \end{aligned} \tag{48}$$

$$\begin{aligned}\left[K_{\psi' u}\right] = \int_\Omega \Big\{ & [B\psi']^T \left[G_{\psi' p}\right]^T [A_{\mathrm{pp}}] [G_{\mathrm{up}}] [Bu] \\ & + [B\psi']^T \left[G_{\psi' p}\right]^T [A_{\mathrm{pn}}] [G_{\mathrm{un}}] [Bu] \\ & + [B\psi']^T \left[G_{\psi' n}\right]^T [A_{\mathrm{np}}] [G_{\mathrm{up}}] [Bu] \\ & + [B\psi']^T \left[G_{\psi' n}\right]^T [A_{\mathrm{nn}}] [G_{\mathrm{un}}] [Bu] \Big\} |\boldsymbol{J}| \mathrm{d}\xi \mathrm{d}\eta, \end{aligned} \tag{49}$$

$$\begin{aligned}\left[K_{\psi' \varphi'}\right] = \int_\Omega \Big\{ & [B\psi']^T \left[G_{\psi' p}\right]^T [A_{\mathrm{pp}}] [G_{\varphi' p}] [B\varphi'] \\ & + [B\psi']^T \left[G_{\psi' p}\right]^T [A_{\mathrm{pn}}] [G_{\varphi' n}] [B\varphi'] \\ & + [B\psi']^T \left[G_{\psi' n}\right]^T [A_{\mathrm{np}}] [G_{\varphi' p}] [B\varphi'] \\ & + [B\psi']^T \left[G_{\psi' n}\right]^T [A_{\mathrm{nn}}] [G_{\varphi' n}] [B\varphi'] \Big\} |\boldsymbol{J}| \mathrm{d}\xi \mathrm{d}\eta, \end{aligned} \tag{50}$$

$$\begin{aligned}\left[K_{\psi'\psi'}\right] = \int_\Omega \Big\{ & [B\psi']^T \left[G_{\psi' p}\right]^T [A_{\mathrm{pp}}] \left[G_{\psi' p}\right] [B\psi'] \\ & + [B\psi']^T \left[G_{\psi' p}\right]^T [A_{\mathrm{pn}}] \left[G_{\psi' n}\right] [B\psi'] \\ & + [B\psi']^T \left[G_{\psi' n}\right]^T [A_{\mathrm{np}}] \left[G_{\psi' p}\right] [B\psi'] \\ & + [B\psi']^T \left[G_{\psi' n}\right]^T [A_{\mathrm{nn}}] \left[G_{\psi' n}\right] [B\psi'] \Big\} |\boldsymbol{J}| \mathrm{d}\xi \mathrm{d}\eta. \end{aligned} \tag{51}$$

The integrals in the domain Ω are numerically computed via points and weights of Gauss. $|\boldsymbol{J}|$ means determinant of the Jacobian matrix.

The integrals in ζ direction are analytically solved, they are four matrices of dimension (9 × 9), which are integrated in each layer l with bounds ζ_t^l and ζ_b^l (coordinates of the top and bottom of each layer l). These four matrices are called $[A_{\mathrm{pp}}]$, $[A_{\mathrm{pn}}]$, $[A_{\mathrm{np}}]$, and $[A_{\mathrm{nn}}]$ and are obtained as summation on the number of layers N_l of each layer contribution: it is an ESL approach and they are simply summed. The matrices are:

Table 14
One-layered orthotropic moderately thin and thick plates with simply supported edges and transverse concentrated load P_z. Maximum transverse no-dimensional displacement $\overline{w}$.

	9P-8N	RM($\chi = 5/6$)	RM	K
$a/h = 100$				
2×2	0.02306	0.02308	0.02306	0.02303
4×4	0.02325	0.02329	0.02325	0.02308
8×8	0.02341	0.02344	0.02340	0.02320
16×16	0.02347	0.02351	0.02346	0.02323
32×32	0.02351	0.02355	0.02350	0.02324
$a/h = 10$				
2×2	0.03638	0.03847	0.03607	0.02303
4×4	0.03919	0.04138	0.03843	0.02308
8×8	0.04265	0.04421	0.04083	0.02320
16×16	0.04716	0.04691	0.04309	0.02323
32×32	0.05246	0.04957	0.04531	0.02324

$$\begin{aligned}[A_{\mathrm{pp}}] &= \sum_{l=1}^{N_l} \int_{\zeta_b^l}^{\zeta_t^l} \left[F_\zeta\right]^T \left[Q_{\mathrm{pp}}^l\right] \left[F_\zeta\right] \mathrm{d}\zeta, \\ [A_{\mathrm{pn}}] &= \sum_{l=1}^{N_l} \int_{\zeta_b^l}^{\zeta_t^l} \left[F_\zeta\right]^T \left[Q_{\mathrm{pn}}^l\right] \left[F_\zeta\right] \mathrm{d}\zeta, \end{aligned} \tag{52}$$

$$\begin{aligned}[A_{\mathrm{np}}] &= \sum_{l=1}^{N_l} \int_{\zeta_b^l}^{\zeta_t^l} \left[F_\zeta\right]^T \left[Q_{\mathrm{np}}^l\right] \left[F_\zeta\right] \mathrm{d}\zeta, \\ [A_{\mathrm{nn}}] &= \sum_{l=1}^{N_l} \int_{\zeta_b^l}^{\zeta_t^l} \left[F_\zeta\right]^T \left[Q_{\mathrm{nn}}^l\right] \left[F_\zeta\right] \mathrm{d}\zeta. \end{aligned} \tag{53}$$

7. Shear and membrane locking correction

As discussed in Polit 1992 and Polit 2008 shear and membrane locking phenomena appear as an excessive stiffness evaluation. In the 9P-8N model the over-stiffness concerns the first six lines of the sub-matrix $[G_{\mathrm{un}}]$ in Eq. (20) and the first six lines of the sub-matrix $[G_{\varphi' n}]$ in Eq. (21) (the first six lines consider the transverse shear strains $\gamma'_{y'z'}$ and $\gamma'_{x'z'}$, the last three lines concern the transverse normal strain $\varepsilon'_{z'z'}$). First six lines of sub-matrix $[G_{\mathrm{un}}]$ give the contribution for $\gamma'_{y'z'}$ and $\gamma'_{x'z'}$ in terms of components u_1, u_2 and u_3; first six lines of sub-matrix $[G_{\varphi n}]$ give the contribution for $\gamma'_{y'z'}$ and $\gamma'_{x'z'}$ in terms of components φ'_1, φ'_2 and φ'_3. In particular the lines which give the over-stiffness in $[G_{\mathrm{un}}]$ and $[G_{\varphi' n}]$ are the first and the fourth ones because they represent the constant part of $\gamma'_{y'z'}$ and $\gamma'_{x'z'}$ which do not equal zero for thin structures. The over-stiffness phenomenon in $[G_{\mathrm{un}}]$ and $[G_{\varphi' n}]$ leads to the shear locking. The membrane locking is due to the over-stiffness in matrix $[G_{\mathrm{up}}]$ of Eq. (17), in it the first three lines concern the normal in-plane strain $\varepsilon'_{x'x'}$, the second three lines concern the normal in-plane strain $\varepsilon'_{y'y'}$ and the last three lines concern the shear in-plane strain $\gamma'_{x'y'}$. Only the fist, fourth and seventh lines need to be corrected because they represent the constant part of $\varepsilon'_{x'x'}$, $\varepsilon'_{y'y'}$ and $\gamma'_{x'y'}$ which do not equal zero for thin structures. In the case of membrane locking only the contribution of u_1, u_2 and u_3 components are considered; the contribution of φ'_1, φ'_2 and φ'_3 components, given by the sub-matrix $[G_{\varphi' p}]$ in Eq. (18), is not relevant.

The first step for the shear locking correction is to write the transverse shear strains as combination of the reduced strains γ_ξ and γ_η:

Table 15
One-layered orthotropic moderately thin and thick plates with clamped edges and transverse concentrated load P_z. Maximum transverse no-dimensional displacement $\overline{w}$.

	9P-8N	RM($\chi = 5/6$)	RM	K
$a/h = 100$				
2×2	0.007156	0.007202	0.007170	0.007012
4×4	0.008442	0.008543	0.008453	0.007820
8×8	0.009342	0.009388	0.009343	0.009032
16×16	0.009409	0.009454	0.009406	0.009148
32×32	0.009443	0.009489	0.009436	0.009164
$a/h = 10$				
2×2	0.02188	0.02438	0.02167	0.007012
4×4	0.02634	0.02876	0.02569	0.007821
8×8	0.02973	0.03158	0.02807	0.009033
16×16	0.03417	0.03427	0.03031	0.009149
32×32	0.03944	0.03692	0.03253	0.009164

Table 16
Three-layered orthotropic (0°/90°/0°) moderately thin and thick plates with simply supported edges and transverse concentrated load P_z. Maximum transverse no-dimensional displacement $\overline{w}$.

	9P-8N	RM ($\chi = 5/6$)	RM	K
$a/h = 100$				
2×2	0.02102	0.02104	0.02102	0.02109
4×4	0.02135	0.02138	0.02135	0.02119
8×8	0.02147	0.02150	0.02146	0.02127
16×16	0.02152	0.02155	0.02152	0.02129
32×32	0.02155	0.02159	0.02154	0.02130
$a/h = 10$				
2×2	0.03350	0.03550	0.03323	0.02109
4×4	0.03739	0.03845	0.03566	0.02119
8×8	0.03963	0.04119	0.03796	0.02128
16×16	0.04407	0.04388	0.04021	0.02130
32×32	0.04935	0.04653	0.04242	0.02130

$$\begin{bmatrix} \gamma'^0_{y'z'} \\ \gamma'^1_{y'z'} \\ \gamma'^2_{y'z'} \\ \gamma'^0_{x'z'} \\ \gamma'^1_{x'z'} \\ \gamma'^2_{y'z'} \end{bmatrix} = [\mathrm{TA}] \begin{bmatrix} \gamma_\xi \\ \gamma_\eta \end{bmatrix} \tag{54}$$

in Eq. (54) only the constant part of $\gamma'_{y'z'}$ and $\gamma'_{x'z'}$ must be corrected (constant part is indicated with superscript 0, linear and quadratic parts in z direction with superscript 1 and 2, respectively), so the matrix [TA] of dimension 6×2, considering the Jacobian of the transformation between local (x',y') and reduced (ξ, η) coordinates, has the following form:

$$[\mathrm{TA}] = \begin{bmatrix} \mathrm{TA}(2,1) & \mathrm{TA}(2,2) \\ 0 & 0 \\ 0 & 0 \\ \mathrm{TA}(1,1) & \mathrm{TA}(1,2) \\ 0 & 0 \\ 0 & 0 \\ 0 & 0 \end{bmatrix}. \tag{55}$$

The reduced strains γ_ξ and γ_η are written by using the five points I and J in pictures (a) and (b) of the Fig. 3:

$$\begin{bmatrix} \gamma_\xi \\ \gamma_\eta \end{bmatrix} = [\mathrm{BC}] \begin{bmatrix} \left(\gamma_{\xi I}\right)_{I=1,5} \\ \left(\gamma_{\eta J}\right)_{J=1,5} \end{bmatrix}, \tag{56}$$

the matrix [BC] of dimension 2×10 contains the interpolation functions $(C\xi_I)_I = I_1, I_5$ and $(C\eta_J)_J = J_1, J_5$ (they are given in explicit form in the Appendix B):

$$[BC] = \begin{bmatrix} C\xi_{I_1} & C\xi_{I_2} & C\xi_{I_3} & C\xi_{I_4} & C\xi_{I_5} & 0 & 0 & 0 & 0 & 0 \\ 0 & 0 & 0 & 0 & 0 & C\eta_{J_1} & C\eta_{J_2} & C\eta_{J_3} & C\eta_{J_4} & C\eta_{J_5} \end{bmatrix}. \tag{57}$$

The reduced shear strains calculated in the five interpolation points can be partially expressed as combination of the u_1, u_2 and u_3 components calculated in the eight nodes k:

$$\begin{bmatrix} (\gamma_{\xi I})_{I=1,5} \\ (\gamma_{\eta J})_{J=1,5} \end{bmatrix} = [\mathrm{PC_u}] \begin{bmatrix} (u_1)_{k=1,8} \\ (u_2)_{k=1,8} \\ (u_3)_{k=1,8} \end{bmatrix}, \tag{58}$$

therefore the matrix $[\mathrm{PC_u}]$ has dimension 10×24 and its structure for a generic node k and for points (I, J) is:

$$[\mathrm{PC_u}]_{I,J,k} = \begin{bmatrix} \vec{a}_\xi \cdot \vec{e}_1 N_{k,\xi} & \vec{a}_\xi \cdot \vec{e}_2 N_{k,\xi} & \vec{a}_\xi \cdot \vec{e}_3 N_{k,\xi} \\ \vec{a}_\xi \cdot \vec{e}_1 N_{k,\eta} & \vec{a}_\xi \cdot \vec{e}_2 N_{k,\eta} & \vec{a}_\xi \cdot \vec{e}_3 N_{k,\eta} \end{bmatrix}. \tag{59}$$

The reduced shear strains calculated in the five interpolation points can also be partially expressed as combination of the φ'_1 and φ'_2 components calculated in the eight nodes k:

$$\begin{bmatrix} (\gamma_{\xi I})_{I=1,5} \\ (\gamma_{\eta J})_{J=1,5} \end{bmatrix} = [\mathrm{PC}_{\varphi'}] \begin{bmatrix} (\varphi'_1)_{k=1,8} \\ (\varphi'_2)_{k=1,8} \end{bmatrix}, \tag{60}$$

therefore the matrix $[\mathrm{PC}_{\varphi'}]$ has dimension 10×16 and its structure for a generic node k and for points (I, J) is:

$$[\mathrm{PC}_{\varphi'}]_{I,J,k} = \begin{bmatrix} \vec{a}_\xi \cdot \vec{a}_1 N_k & \vec{a}_\xi \cdot \vec{a}_2 N_k \\ \vec{a}_\eta \cdot \vec{a}_1 N_k & \vec{a}_\eta \cdot \vec{a}_2 N_k \end{bmatrix}. \tag{61}$$

By using Eqs. (54)–(61), it is possible to obtain the shear locking correction matrices for the constant part of u_1, u_2 and u_3 components ($[\mathrm{CS}_{u^0}]$ of dimension 6×24) and for the constant part of φ'_1 and φ'_2 components ($[\mathrm{CS}_{\varphi'^0}]$ of dimension 6×16):

$$[\mathrm{CS}_{u^0}] = [\mathrm{TA}]\,[\mathrm{BC}][\mathrm{PC_u}], \tag{62}$$

$$\left[\mathrm{CS}_{\varphi'^0}\right] = [\mathrm{TA}]\,[\mathrm{BC}]\left[\mathrm{PC}_{\varphi'}\right]. \tag{63}$$

For the membrane locking correction, the first step is to write the normal in-plane strains and the shear in-plane strain as combinations of the reduced strains $\varepsilon_{\xi\xi}$, $\varepsilon_{\eta\eta}$ and $\gamma_{\xi\eta}$:

$$\begin{bmatrix} \varepsilon'^0_{x'x'} \\ \varepsilon'^1_{x'x'} \\ \varepsilon'^2_{x'x'} \\ \varepsilon'^0_{y'y'} \\ \varepsilon'^1_{y'y'} \\ \varepsilon'^2_{y'y'} \\ \gamma'^0_{x'y'} \\ \gamma'^1_{x'y'} \\ \gamma'^2_{x'y'} \end{bmatrix} = [\mathrm{TA}m] \begin{bmatrix} \varepsilon_{\xi\xi} \\ \varepsilon_{\eta\eta} \\ \gamma_{\xi\eta} \end{bmatrix} \tag{64}$$

in Eq. (64) only the constant part of $\varepsilon'_{x'x'}$, $\varepsilon'_{y'y'}$ and $\gamma'_{x'y'}$ must be corrected (constant part are indicated with superscript 0), so the matrix [TAm] of dimension 9×3 has the following form (see also matrix [TA] in Eq. (55)):

Table 17
Three-layered orthotropic (0°/90°/0°) moderately thin and thick plates with clamped edges and transverse concentrated load P_z. Maximum transverse non-dimensional displacement $\overline{w}$.

	9P-8N	RM ($\chi = 5/6$)	RM	K
$a/h = 100$				
2×2	0.007146	0.007190	0.007160	0.007012
4×4	0.007869	0.007936	0.007875	0.007466
8×8	0.008345	0.008386	0.008345	0.008104
16×16	0.008395	0.008436	0.008392	0.008164
32×32	0.008425	0.008467	0.008419	0.008173
$a/h = 10$				
2×2	0.02049	0.02268	0.02029	0.007012
4×4	0.02302	0.02601	0.02322	0.007467
8×8	0.02706	0.02878	0.02554	0.008105
16×16	0.03145	0.03145	0.02777	0.008164
32×32	0.03669	0.03410	0.02998	0.008173

By using Eqs. (64)–(69), it is possible to obtain the membrane locking correction matrix for the constant part of u_1, u_2 and u_3 components denoted as $[\mathrm{CM}_{u^0}]$ (its dimension is 9×24):

$$[CM_{u^0}] = [\mathrm{TA}m]\,[BCm][PCm]. \tag{70}$$

The shear locking is corrected when the first and fourth lines of the matrix $[\mathrm{CS}_{u^0}]$ are substituted in the first and fourth lines of the (9×24) matrix given by the product $[G_{\mathrm{un}}][Bu]$, and when the first and fourth lines of the matrix $[\mathrm{CS}_{\varphi^0}]$ are substituted in the first and fourth lines of the (9×24) matrix given by the product $[G_{\varphi' n}][B\varphi']$ (in this case the contribution given by the component φ'_3 is not considered). The membrane locking is corrected when the first, fourth and seventh lines of the matrix $[\mathrm{CM}_{u^0}]$ are substituted in the relative lines of the (9×24) matrix given by the product $[G_{\mathrm{up}}][Bu]$.

$$[\mathrm{TA}m] = \begin{bmatrix} \mathrm{TA}(1,1)^2 & \mathrm{TA}(1,2)^2 & \mathrm{TA}(1,1)\mathrm{TA}(1,2) \\ 0 & 0 & 0 \\ 0 & 0 & 0 \\ \mathrm{TA}(2,1)^2 & \mathrm{TA}(2,2)^2 & \mathrm{TA}(2,1)\mathrm{TA}(2,2) \\ 0 & 0 & 0 \\ 0 & 0 & 0 \\ 2\mathrm{TA}(1,1)\mathrm{TA}(2,1) & 2\mathrm{TA}(1,2)\mathrm{TA}(2,2) & \mathrm{TA}(1,1)\mathrm{TA}(2,2) + \mathrm{TA}(1,2)\mathrm{TA}(2,1) \end{bmatrix} \tag{65}$$

The reduced strains $\varepsilon_{\xi\xi}$ and $\varepsilon_{\eta\eta}$ are written by using the five points I and J in pictures (a) and (b) of the Fig. 3. The reduce strain $\gamma_{\xi\eta}$ is written by using the four points M in picture (c) of the Fig. 3:

$$\begin{bmatrix} \varepsilon_{\xi\xi} \\ \varepsilon_{\eta\eta} \\ \gamma_{\xi\eta} \end{bmatrix} = [\mathrm{BC}m] \begin{bmatrix} (\varepsilon_{\xi\xi I})_{I=1,5} \\ (\varepsilon_{\eta\eta J})_{J=1,5} \\ (\gamma_{\xi\eta M})_{M=1,4} \end{bmatrix}, \tag{66}$$

the matrix $[\mathrm{BC}m]$ of dimension 3×14 contains the interpolation functions $(C\xi_I)_I = I_1, I_5$, $(C\eta_J)_J = J_1, J_5$ and $(C\xi\eta_M)_M = M_1, M_4$ (they are given in explicit form in the Appendix B):

$$[\mathrm{BC}m] = \begin{bmatrix} C\xi_{I_1} & C\xi_{I_2} & C\xi_{I_3} & C\xi_{I_4} & C\xi_{I_5} & 0 & 0 & 0 & 0 & 0 & 0 & 0 & 0 & 0 \\ 0 & 0 & 0 & 0 & 0 & C\eta_{J_1} & C\eta_{J_2} & C\eta_{J_3} & C\eta_{J_4} & C\eta_{J_5} & 0 & 0 & 0 & 0 \\ 0 & 0 & 0 & 0 & 0 & 0 & 0 & 0 & 0 & 0 & C\xi\eta_{M_1} & C\xi\eta_{M_2} & C\xi\eta_{M_3} & C\xi\eta_{M_4} \end{bmatrix}. \tag{67}$$

The reduced in-plane normal and shear strains calculated in the five and four interpolation points, respectively, can be partially expressed as combination of the u_1, u_2 and u_3 components calculated in the eight nodes k:

$$\begin{bmatrix} \left(\varepsilon_{\xi\xi I}\right)_{I=1,5} \\ (\varepsilon_{\eta\eta J})_{J=1,5} \\ \left(\gamma_{\xi\eta M}\right)_{M=1,4} \end{bmatrix} = [\mathrm{PC}m] \begin{bmatrix} (u_1)_{k=1,8} \\ (u_2)_{k=1,8} \\ (u_3)_{k=1,8} \end{bmatrix}, \tag{68}$$

therefore the matrix $[\mathrm{PC}m]$ has dimension 14×24 and its structure for a generic node k and for points (I, J, M) is:

$$[\mathrm{PC}m]_{I,J,M,k} = \begin{bmatrix} \vec{a}_\xi \cdot \vec{e}_1 N_{k,\xi} & \vec{a}_\xi \cdot \vec{e}_2 N_{k,\xi} & \vec{a}_\xi \cdot \vec{e}_3 N_{k,\xi} \\ \vec{a}_\eta \cdot \vec{e}_1 N_{k,\eta} & \vec{a}_\eta \cdot \vec{e}_2 N_{k,\eta} & \vec{a}_\eta \cdot \vec{e}_3 N_{k,\eta} \\ \vec{a}_\eta \cdot \vec{e}_1 N_{k,\xi} + \vec{a}_\xi \cdot \vec{e}_1 N_{k,\eta} & \vec{a}_\eta \cdot \vec{e}_2 N_{k,\xi} + \vec{a}_\xi \cdot \vec{e}_2 N_{k,\eta} & \vec{a}_\eta \cdot \vec{e}_3 N_{k,\xi} + \vec{a}_\xi \cdot \vec{e}_3 N_{k,\eta} \end{bmatrix}. \tag{69}$$

8. Results

The results given in this section are organized as follows: the 9P-8N model is preliminary validated for thin isotropic one-layered plates (simply supported or clamped sides) with a concentrated load and for the one-layered isotropic pinched cylinder. The effects of both shear and membrane locking are also evaluated in such cases. After this validation, the same structures with a bigger thickness are analyzed in order to demonstrate the importance of the use of a refinement model for such cases. In the second part of this section, the 9P-8N model is also validated for orthotropic composite one-layered and multilayered plates and shells (the same geometries proposed for the isotropic cases). After this validation, the importance of the refined 9P-8N shell model is demonstrated for the cases of thick and composite structures.

In the given tables and figures, the proposed shell model with both shear and membrane locking corrections is indicated with the acronym 9P-8N. When both locking corrections are discarded the model is indicated as 9P-8N(iso). In the convergence studies if only the shear locking correction (SL) is included the employed acronym is 9P-8N(SL). From the refined model 9P-8N it is possible to obtain the classical ones, such as the Reissner-Mindlin (RM) and the

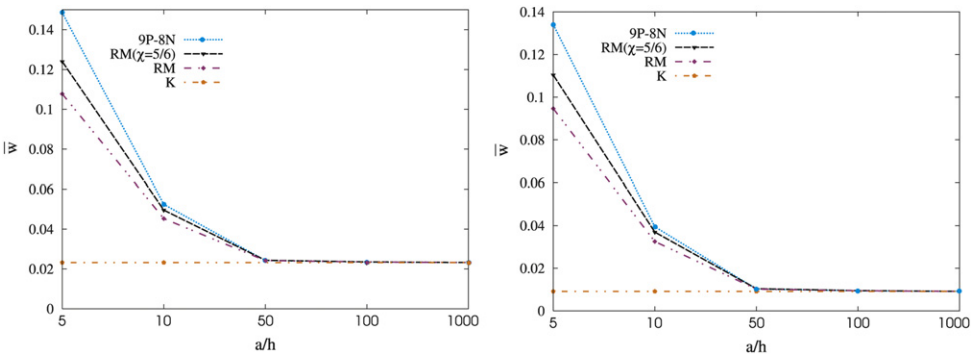

Fig. 8. Convergence study (mesh 32 × 32) for the one-layered orthotropic plate with simply supported edges (left) and clamped edges (right).

Kirchhoff (K) model, via a penalty technique. The RM model is obtained by discarding the quadratic terms in the in-plane displacement components and both the linear and quadratic terms in the transverse displacement component (the relative terms in the stiffness matrix are multiplied for an infinite coefficient $C = 10^{20}$). The K model is obtained from the RM model by penalizing the elastic coefficients Q_{ij} related to the transverse shear strains (use of an infinite shear correction factor $\chi = 10^5$).

8.1. Preliminary assessments for isotropic homogeneous structures

As preliminary results the one-layered isotropic plate, with a concentrated load $P_z = 4N$ in its middle in the z direction, is considered (see Fig. 4). Such a square ($a = b = 10$ m) plate with thickness value $h = 0.01$ m is investigated for two different boundary conditions: simple supported and clamped edges. The material data are Young modulus $E = 10.92$ GPa and Poisson ratio $\nu = 0.3$. The plate is very thin (thickness ratio $a/h = 1000$) and as reference solution we can consider the analytical one based on Kirchhoff theory as proposed in Batoz and Dhatt 1992: for the simply supported plate the maximum transverse displacement is $w_{\max} = 0.0116 P_z a^2/D = 4.64 \times 10^{-3}$ m and for the clamped one is $w_{\max} = 0.0056 P_z a^2/D = 2.24 \times 10^{-3}$ m where $D = Eh^3/12(1-\nu^2)$. Table 1 gives the maximum transverse displacement $w_{\max}$ in the middle of the simply supported plate; when the shear locking phenomenon is corrected the 9P-8N model gives the reference result for a very simple mesh (2 × 2), when the shear locking is not corrected the 9P-8N(iso) model needs a very refined mesh to obtain a good value, however even when a 32 × 32 mesh is considered the value given in Batoz and Dhatt 1992 is not perfectly achieved. RM (Reissner-Mindlin) and K (Kirchhoff) models are obtained via penalty technique from the 9P-8N model (the shear locking correction is included), the plate is very thin and isotropic made, therefore the reference solution (Batoz and Dhatt, 1992) is also obtained by these classical models. The same results and considerations are valid for the clamped isotropic plate in Table 2, all the conclusions just made for the simply supported plate are here confirmed for the clamped case. However, these boundary conditions are more complicated than the simply supported case, so the 9P-8N model needs a refined mesh (16 × 16) to obtain the correct result (Batoz and Dhatt, 1992). RM and K models are very efficient because the plate is thin and isotropic. Fig. 5 gives the evaluation of the 9P-8N and 9P-8N(iso) models, when the mesh is increased, with respect to the analytical reference solution (Batoz and Dhatt, 1992) (both simply supported and clamped plates). When the shear locking is opportunely corrected (9P-8N) the reference solution is immediately obtained with a coarse mesh, without shear locking correction (9P-8N(iso) model) a refined mesh is requested and as just discussed for Tables 1 and 2 the correct result is not perfectly achieved (a further refinement of the mesh should give the correct result).

As second preliminary investigation the one-layered pinched cylindrical shell is considered with a concentrated load $P_z = 1N$ (see Fig. 6). In order to investigate such a case only the area A-B-C-D is considered for symmetry considerations (see Fig. 6) with a concentrated load $P_z/4 = -0.25N$. The shell is made of an isotropic material with Young modulus $E = 30$ GPa and Poisson ratio $\nu = 0.3$. The length is $L = 6$ m and the radius is $R = 3$ m. The shell is moderately thin ($R/h = 100$) because the global thickness is $h = 0.03$ m. An analytical reference solution given in the open literature has been proposed by Flügge 1973: maximum transverse displacement in the point C $(w_{\max})_C = -0.18248 \times 10^{-6}$ m and maximum longitudinal displacement in the point D $(v_{\max})_D = 0.45711 \times 10^{-8}$ m. This analytical solution is based on Kirchhoff hypothesis and it does not consider the transverse shear deformations. In this case the inclusion of the transverse shear effects is much more important than the plate case because the thickness ratio is 100 and not 1000, and because the curvature produces a shear effect even if a concentrated load is considered. This aspect is confirmed by several convergence solutions proposed in the open literature which are obtained with models based on Reissner-Mindlin hypotheses or other refined theories: see for example the result by Reddy 2004 ($(w_{\max})_C = -0.18661 \times 10^{-6}$ m based on the well-known Reddy theory), that by Cho and Roh 2003 ($(w_{\max})_C = -0.18541 \times 10^{-6}$ m based on the Reissner-Mindlin theory) and that by Zhao et al. 2008 ($(w_{\max})_C = -0.18663 \times 10^{-6}$ m based on the Reissner-Mindlin theory). Table 3 proposes the 9P-8N model with both shear and membrane locking corrections, it is compared with the 9P-8N(SL) model where only the shear locking is corrected and with the 9P-8N(iso) model where no locking corrections have been introduced. In the case of shell geometry there are both shear and membrane locking (for the plate geometry only the shear locking phenomenon appears), the major contribution is given by the shear locking correction but the membrane locking correction permits a further refinement. This fact is confirmed by the Fig. 7 which gives the evaluation of the maximum transverse displacement (left part) and maximum longitudinal displacement (right part) when the mesh is increased: a great contribution is given by the shear locking correction which improves in a consistent way the results, a further improvement is given by the membrane locking correction. The analytical result given by Flügge 1973 is based on Kirchhoff theory, so the 9P-8N model gives a bigger transverse displacement because of the inclusion of the transverse shear deformability. This fact is confirmed by the RM model and by the analysis proposed by Reddy 2004 and Zhao et al. 2008. When we consider a K model, a smaller transverse displacement is obtained and it is very close to Flügge 1973 result

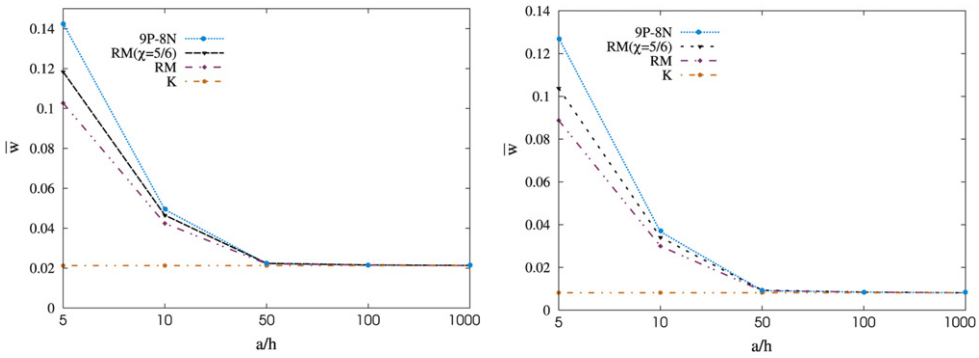

Fig. 9. Convergence study (mesh 32 × 32) for the three-layered orthotropic (0°/90°/0°) plate with simply supported edges (left) and clamped edges (right).

(K model and Flügge results use the same theory based on Kirchhoff hypothesis, the first is a numerical approach and the second one is an analytical approach), this confirms that the best values are obtained when the transverse shear effects are included in the FE models. All the considerations made for the transverse displacement proposed in Table 3 are confirmed for the longitudinal displacement given in Table 4: the importance of the locking corrections is confirmed but for the longitudinal displacement component the inclusion of the transverse shear effect is not so important as in the transverse displacement case (see the results given by the K model).

8.2. Thick and moderately thick isotropic homogeneous structures

After the validation of the 9P-8N model for thin isotropic structures, in this section its importance for thick and moderately thick cases is demonstrated. For this aim the same simple supported and clamped plates are considered (same geometry, loading conditions and materials) but with thickness h equals 0.1 m and 1 m (this means thickness ratio $a/h = 100$ and $a/h = 10$, respectively). These moderately thick plates have been proposed in order to demonstrate the importance of both transverse shear effects and through-the-thickness stretching. Table 5 proposes the maximum transverse displacement for moderately thin ($a/h = 100$) and thick ($a/h = 10$) isotropic simply supported plate. 9P-8N model can be considered as the reference solution because it includes those effects which appear when a moderately thick structure is considered. For $a/h = 100$ RM and K models give satisfactory values even if the K model gives a small error (4.64 vs. 4.67 if a 32 × 32 mesh is considered). When the plate is thick ($a/h = 10$), the K model is completely inadequate (it does not consider the transverse shear effects and the through-the-thickness deformation). The RM model gives some improvements (it includes the transverse shear effects) but it does not give the correct result (even if a shear correction factor χ is applied). These results and considerations are also proposed for the same plate in the case of clamped edges in Table 6, no further comments originate: the change of boundary conditions does not modify the results and their discussion, the K model remains totally inadequate for thick plates and the RM model (even if a shear correction factor χ is applied) does not achieve the correct result.

8.3. Assessments for orthotropic composite structures

The assessments proposed in this section permit to validate the 9P-8N model for orthotropic composite structures. The same plates considered for the isotropic cases are investigated (square plate with $a = b = 10$ m, transverse load $P_z = 4N$, thickness value $h = 0.01$ m, both cases of simply supported and clamped edges). The considered material has longitudinal Young modulus $E_L = 25$ GPa and the other two transverse Young modulus $E_T = 1$ GPa, the shear modulus values are $G_{LT} = G_{TT} = 0.5$ GPa and the Poisson ratio is $\nu_{LT} = \nu_{TT} = 0.25$. For this thin plates ($a/h = 1000$) Bhaskar and Kaushik (2004) give exact solutions for the following four cases in terms of maximum no-dimensional transverse displacement $\overline{w} = E_T h^3 w_{max}/P_z a^4$: $\overline{w} = 0.02324$ for the one-layered simply supported plate (fiber orientation 0°) in Table 7; $\overline{w} = 0.009167$ for the one-layered clamped plate (fiber orientation 0°) in Table 8; $\overline{w} = 0.02131$ for the three-layered simply supported plate (fiber orientation 0°/90°) in Table 9; $\overline{w} = 0.008175$ for the three-layered clamped plate (fiber orientation 0°/90°) in Table 10. Tables 7–10 demonstrate as the 9P-8N model is completely adequate to describe the behavior of a composite plate for different lamination sequences and boundary conditions, with a refined mesh it perfectly gives the analytical results proposed by Bhaskar and Kaushik 2004. However the plate is very thin ($a/h = 1000$), and this fact also permits to obtain quite satisfactory analysis with classical models such as the K and RM ones.

The second assessment is provided for the same geometry of the cylinder proposed for the isotropic case ($L = 6$ m, $R = 3$ m, $h = 0.03$ m, $P_z = 1N$, $R/h = 100$). The considered orthotropic composite material has the following properties: longitudinal Young modulus $E_L = 40$ MPa, transverse Young modulus $E_T = 1$ MPa, Poisson ratio $\nu_{LT} = \nu_{TT} = 0.25$ and shear modulus $G_{LT} = 0.6$ MPa and $G_{TT} = 0.5$ MPa. The cases proposed by Jones 2002 consider one orthotropic layer oriented in the axial direction (90°) (see Table 11), one orthotropic layer oriented in the circumferential direction (0°) (see Table 12) and a three-layered configuration with lamination sequence 90°/0°/90° (see Table 13). Jones 2002 provides the maximum transverse displacement in the point C in no-dimensional form $\overline{w} = E_L h w_{max}/P_z$. The given results are those based on Flügge 1973 theory extended to multilayered orthotropic cylinders and the shear deformable solution, as proposed by Sanders 1959, extended to multilayered orthotropic cylinders. These two solutions are provided in analytical form, for comparison purposes a shear deformable shell FE solution (based on the ABAQUS element S8R5) is also given. The shell case is more complicated than the relative plate cases proposed in the first part of this section, in fact the pinched load matched with the curvature remarks the importance of the transverse shear effects. In Table 11 the 9P-8N model is in accordance with the shear deformable solution proposed by Sanders, the RM model gives results very close to the ABAQUS element because both consider the Reissner-Mindlin hypothesis, the K model is very close to Flügge 1973 result because both models are based on Kirchhoff hypothesis. By considering the results given by Sanders and by the 9P-8N model with a 32 × 32 mesh, it is evident as the inclusion of the transverse

shear effects is fundamental. These considerations are also valid if the lamination sequence changes as proposed in Tables 12 and 13.

8.4. Thick and thin orthotropic composite structures

In the previous section the 9P-8N model has been validated for orthotropic composite structures. Here, its importance for thick and moderately thick composite structures is demonstrated by considering the same previously proposed composite plates but with thickness ratios $a/h = 100$ and $a/h = 10$. Tables 14 and 15 propose the maximum transverse displacement $\overline{w}$ for the simply supported and clamped one-layered orthotropic plates, respectively. Tables 16 and 17 consider the same results for simply supported and clamped three-layered composite plates, respectively. It is evident as for each lamination sequence and boundary conditions the K model is totally inadequate, it can be used only if the plate is thin. Some improvements are obtained if an RM model is considered (in particular if a shear correction factor χ is introduced), but such models give an error if thick and moderately thick plates are considered. All these considerations are clearly reported in Figs. 8 and 9. Fig. 8 gives the convergence study (the employed mesh is 32×32) for the one-layered orthotropic plate: for both simply supported and clamped conditions the use of the 9P-8N model appears suitable for thickness ratios a/h from 5 to 50, the RM model gives some improvements with respect to the K model but until to $a/h = 20$ it is quite distant from the 9P-8N model (even if a shear correction factor χ is introduced). These considerations are confirmed and the use of the 9P-8N model remains suitable for the three-layered cases proposed in Fig. 9: from the convergence study the limitations of classical theories (RM and K models) is clearly indicated.

A further validation of the 9P-8N model is given in Table 18 where the proposed model is compared with some 3D reference solutions in terms of displacements and stresses. The investigated benchmark is the well-known shell proposed by Ren 1987, the cylindrical shell panel is simply supported with geometry as indicated in Fig. 10 where the radii of curvature are $R_\alpha = 10$ m and infinite R_β, the dimensions are $a = \pi/3 R_\alpha = 10.47197551$ m and $b = 1$ m. Ren 1987 considers a transverse mechanical load at the top in the form $P_z = P_z^t \sin(m\pi x/a)$ with amplitude $P_z^t = 1$psi and wave numbers $m = 1$ and $n = 0$ (cylindrical bending). The two layers of the same thickness $h_1 = h_2 = h/2$ are in composite material with lamination sequence 90°/0° (longitudinal and transverse Young moduli $E_L = 25 \times 10^6$ psi and $E_T = 1 \times 10^6$ psi, shear moduli $G_{LT} = 0.5 \times 10^6$ psi and $G_{TT} = 0.2 \times 10^6$ psi, Poisson ratios $\nu_{LT} = \nu_{TT} = 0.25$), the 3D results by Ren 1987 are given in terms of no-dimensional transverse displacement $\overline{w} = 10 E_T w / P_z^t h (R_\alpha/h)^4$, no-dimensional in-plane normal stresses $(\overline{\sigma}_{xx}, \overline{\sigma}_{yy}) = (\sigma_{xx}, \sigma_{yy})/P_z^t (R_\alpha/h)^2$ and no-dimensional transverse shear stress $\overline{\sigma}_{xz} = \sigma_{xz}/P_z^t (R_\alpha/h)$. The transverse displacements and the in-plane normal stresses are evaluated in the middle of the shell (point A in Fig. 10), transverse shear stresses are evaluated in the middle of the rectilinear side of the shell (point B in Fig. 10). These results are given in the first part of Table 18 for thickness ratios R_α/h equal 10 and 500, 9P-8N model is compared with the 3D solution by Ren 1987. A 7-parameter model (here called as 7P-8N), with linear expansion for in-plane displacements and quadratic expansion for the transverse displacement (obtained from the 9P-8N model via a typical penalty technique as discussed in the introduction of Section 8), is also proposed to remark the differences in the case of non-symmetric lamination. The LD4 model is given as quasi-3D solution, it is an analytical solution based on Carrera's Unified Formulation (CUF) (Carrera, 2002) which is in layer wise form with fourth order of expansion in the thickness direction for each displacement component. LD4 model gives the 3D solution for each thickness ratio and for each investigated variable, therefore it can be used as reference quasi-3D solution in the second part of the Table 18 where a bi-sinusoidal load $P_z = P_z^t \sin(m\pi x/a)\sin(n\pi y/b)$ with wave numbers $m = n = 1$ is applied at the top of the same cylindrical shell panel. In this case the advantages of the 9P-8N model are more evident. The employed mesh for the FE models is 64×32 and an eight node element is considered (8N), this mesh permits a quasi-3D response in the case of moderately thick and thin shells. For the cylindrical bending cases (thick and thin shell) the values for transverse displacement and in-plane normal stresses are satisfactory for both 9P-8N and 7P-8N models, 9P-8N model works better than the 7P-8N one for the transverse shear stress evaluation even if a further refinement of the 9P-8N model

Table 18
Two-layered orthotropic (90°/0°) thick and thin cylindrical shell panel with simply supported edges and transverse load P_z (sinusoidal and bi-sinusoidal cases). No-dimensional transverse displacement $\overline{w}$, in-plane normal stresses $\overline{\sigma}_{xx}$ and $\overline{\sigma}_{yy}$, and transverse shear stress $\overline{\sigma}_{xz}$.

	$\overline{w}$ (0)	$\overline{\sigma}_{xx}$ (h/2)	$\overline{\sigma}_{yy}$ (h/2)	$\overline{\sigma}_{xz}$ (h/4)
$R_\alpha/h = 10$ ($m = 1$, $n = 0$)				
3D (Ren, 1987)	0.493	2.245	0.0250	0.879
Quasi-3D (Carrera, 2002)	0.493	2.245	0.0249	0.880
9P-8N	0.486	2.190	0.0190	0.612
7P-8N	0.484	2.200	0.0190	0.559
$R_\alpha/h = 500$ ($m = 1$, $n = 0$)				
3D (Ren, 1987)	0.399	2.153	0.0215	0.865
Quasi-3D (Carrera, 2002)	0.399	2.153	0.0215	0.865
9P-8N	0.399	2.153	0.0223	0.594
7P-8N	0.399	2.154	0.0223	0.541
$R_\alpha/h = 10$ ($m = 1$, $n = 1$)				
Quasi-3D (Carrera, 2002)	0.346×10^{-3}	0.0200	0.00902	0.00605
9P-8N	0.313×10^{-3}	0.0176	0.00507	0.00508
7P-8N	0.306×10^{-3}	0.0163	0.00350	0.00683
$R_\alpha/h = 500$ ($m = 1$, $n = 1$)				
Quasi-3D (Carrera, 2002)	0.327×10^{-5}	0.00338	0.000269	0.00131
9P-8N	0.327×10^{-5}	0.00338	0.000267	0.00145
7P-8N	0.327×10^{-5}	0.00338	0.000268	0.00183

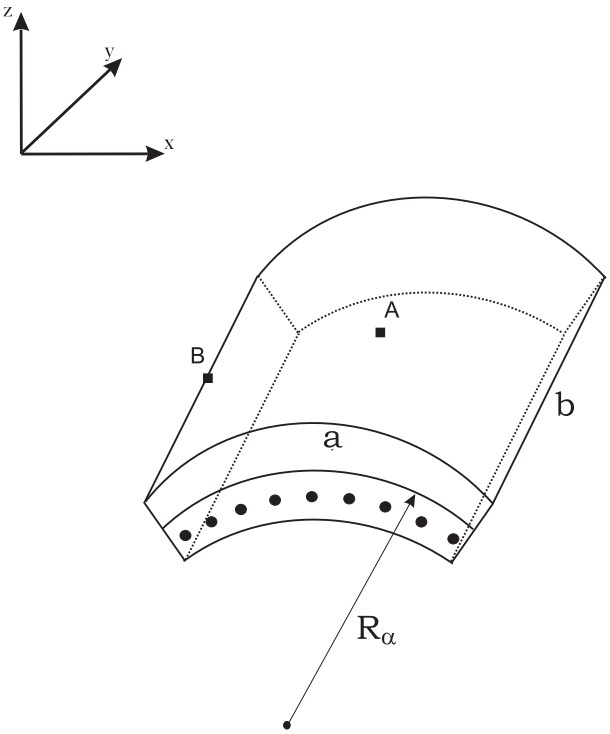

Fig. 10. Two-layered orthotropic (90°/0°) cylindrical shell panel proposed by Ren. Points A and B where the variables are evaluated.

could be considered in the future for such investigations. The importance of the 9P-8N model is also shown for the in-plane normal stresses and transverse displacements (in particular for the thick geometry) when a bi-sinusoidal load is applied. The quadratic terms of expansion in the in-plane displacement components are important for the coupling between bending and membrane strains when a non-symmetric lamination is considered.

9. Conclusions

The 9P-8N is a refined finite element shell model free of both shear and membrane locking phenomena, and it is very promising for the analysis of isotropic and orthotropic composite structures (both plate and shell geometries). The model uses an eight-nodes element with nine degrees of freedom for each node, these nine parameters lead to a quadratically expansion for the three displacement components in the thickness direction. This feature permits to analyze thick and moderately thick isotropic and orthotropic composite structures where both transverse shear and through-the-thickness effects must be included, and to consider the model free of Poisson thickness locking. Comparisons with classical models such those based on Kirchhoff or Reissner-Mindlin hypothesis have demonstrated the advantages of the proposed kinematics. The results are satisfactory for several geometries, boundary conditions, embedded materials and lamination sequences.

Appendix A

$$
\begin{aligned}
A_1 &= t_{11}^2 J_{11}^* + t_{11}t_{12}J_{21}^* + t_{11}t_{13}J_{31}^*, \quad B_1 = t_{11}^2 J_{12}^* + t_{11}t_{12}J_{22}^* + t_{11}t_{13}J_{32}^*,\\
C_1 &= t_{12}t_{11}J_{11}^* + t_{12}^2 J_{21}^* + t_{12}t_{13}J_{31}^*, \quad D_1 = t_{12}t_{11}J_{12}^* + t_{12}^2 J_{22}^* + t_{12}t_{13}J_{32}^*,\\
E_1 &= t_{13}t_{11}J_{11}^* + t_{13}t_{12}J_{21}^* + t_{13}^2 J_{31}^*, \quad F_1 = t_{13}t_{11}J_{12}^* + t_{13}t_{12}J_{22}^* + t_{13}^2 J_{32}^*,\\
A_2 &= t_{21}^2 J_{11}^* + t_{21}t_{22}J_{21}^* + t_{21}t_{23}J_{31}^*, \quad B_2 = t_{21}^2 J_{12}^* + t_{21}t_{22}J_{22}^* + t_{21}t_{23}J_{32}^*,\\
C_2 &= t_{22}t_{21}J_{11}^* + t_{22}^2 J_{21}^* + t_{22}t_{23}J_{31}^*, \quad D_2 = t_{22}t_{21}J_{12}^* + t_{22}^2 J_{22}^* + t_{22}t_{23}J_{32}^*,\\
E_2 &= t_{23}t_{21}J_{11}^* + t_{23}t_{22}J_{21}^* + t_{23}^2 J_{31}^*, \quad F_2 = t_{23}t_{21}J_{12}^* + t_{23}t_{22}J_{22}^* + t_{23}^2 J_{32}^*,\\
A_3 &= 2t_{11}t_{21}J_{11}^* + t_{21}t_{12}J_{21}^* + t_{21}t_{13}J_{31}^* + t_{11}t_{22}J_{21}^* + t_{11}t_{23}J_{31}^*,\\
B_3 &= 2t_{11}t_{21}J_{12}^* + t_{21}t_{12}J_{22}^* + t_{21}t_{13}J_{32}^* + t_{11}t_{22}J_{22}^* + t_{11}t_{23}J_{32}^*,\\
C_3 &= t_{12}t_{21}J_{11}^* + 2t_{12}t_{22}J_{21}^* + t_{12}t_{23}J_{31}^* + t_{22}t_{13}J_{31}^* + t_{11}t_{22}J_{11}^*,\\
D_3 &= t_{12}t_{21}J_{12}^* + 2t_{12}t_{22}J_{22}^* + t_{12}t_{23}J_{32}^* + t_{22}t_{13}J_{32}^* + t_{11}t_{22}J_{12}^*,\\
E_3 &= t_{13}t_{21}J_{11}^* + t_{13}t_{22}J_{21}^* + 2t_{13}t_{23}J_{31}^* + t_{12}t_{23}J_{21}^* + t_{11}t_{23}J_{11}^*,\\
F_3 &= t_{13}t_{21}J_{12}^* + t_{13}t_{22}J_{22}^* + 2t_{13}t_{23}J_{32}^* + t_{12}t_{23}J_{22}^* + t_{11}t_{23}J_{12}^*,\\
A_4 &= 2t_{21}t_{31}J_{11}^* + t_{31}t_{22}J_{21}^* + t_{31}t_{23}J_{31}^* + t_{21}t_{32}J_{21}^* + t_{21}t_{33}J_{31}^*,\\
B_4 &= 2t_{21}t_{31}J_{12}^* + t_{31}t_{22}J_{22}^* + t_{31}t_{23}J_{32}^* + t_{21}t_{32}J_{22}^* + t_{21}t_{33}J_{32}^*,\\
C_4 &= t_{22}t_{31}J_{11}^* + 2t_{22}t_{32}J_{21}^* + t_{22}t_{33}J_{31}^* + t_{32}t_{23}J_{31}^* + t_{21}t_{32}J_{11}^*,\\
D_4 &= t_{22}t_{31}J_{12}^* + 2t_{22}t_{32}J_{22}^* + t_{22}t_{33}J_{32}^* + t_{32}t_{23}J_{32}^* + t_{21}t_{32}J_{12}^*,\\
E_4 &= t_{23}t_{31}J_{11}^* + t_{23}t_{32}J_{21}^* + 2t_{23}t_{33}J_{31}^* + t_{22}t_{33}J_{21}^* + t_{21}t_{33}J_{11}^*,\\
F_4 &= t_{23}t_{31}J_{12}^* + t_{23}t_{32}J_{22}^* + 2t_{23}t_{33}J_{32}^* + t_{22}t_{33}J_{22}^* + t_{21}t_{33}J_{12}^*,\\
A_5 &= 2t_{11}t_{31}J_{11}^* + t_{31}t_{12}J_{21}^* + t_{31}t_{13}J_{31}^* + t_{11}t_{32}J_{21}^* + t_{11}t_{33}J_{31}^*,\\
B_5 &= 2t_{11}t_{31}J_{12}^* + t_{31}t_{12}J_{22}^* + t_{31}t_{13}J_{32}^* + t_{11}t_{32}J_{22}^* + t_{11}t_{33}J_{32}^*,\\
C_5 &= t_{12}t_{31}J_{11}^* + 2t_{12}t_{32}J_{21}^* + t_{12}t_{33}J_{31}^* + t_{32}t_{13}J_{31}^* + t_{11}t_{32}J_{11}^*,\\
D_5 &= t_{12}t_{31}J_{12}^* + 2t_{12}t_{32}J_{22}^* + t_{12}t_{33}J_{32}^* + t_{32}t_{13}J_{32}^* + t_{11}t_{32}J_{12}^*,\\
E_5 &= t_{13}t_{31}J_{11}^* + t_{13}t_{32}J_{21}^* + 2t_{13}t_{33}J_{31}^* + t_{12}t_{33}J_{21}^* + t_{11}t_{33}J_{11}^*,\\
F_5 &= t_{13}t_{31}J_{12}^* + t_{13}t_{32}J_{22}^* + 2t_{13}t_{33}J_{32}^* + t_{12}t_{33}J_{22}^* + t_{11}t_{33}J_{12}^*,\\
A_6 &= t_{31}^2 J_{11}^* + t_{31}t_{32}J_{21}^* + t_{31}t_{33}J_{31}^*, \quad B_6 = t_{31}^2 J_{12}^* + t_{31}t_{32}J_{22}^* + t_{31}t_{33}J_{32}^*,\\
C_6 &= t_{32}t_{31}J_{11}^* + t_{32}^2 J_{21}^* + t_{32}t_{33}J_{31}^*, \quad D_6 = t_{32}t_{31}J_{12}^* + t_{32}^2 J_{22}^* + t_{32}t_{33}J_{32}^*,\\
E_6 &= t_{33}t_{31}J_{11}^* + t_{33}t_{32}J_{21}^* + t_{33}^2 J_{31}^*, \quad F_6 = t_{33}t_{31}J_{12}^* + t_{33}t_{32}J_{22}^* + t_{33}^2 J_{32}^*,\\
G_1 &= t_{11}^2 J_{13}^* + t_{11}t_{12}J_{23}^* + t_{11}t_{13}J_{33}^*, \quad H_1 = t_{11}t_{12}J_{13}^* + t_{12}^2 J_{23}^* + t_{12}t_{13}J_{33}^*,\\
I_1 &= t_{11}t_{13}J_{13}^* + t_{12}t_{13}J_{23}^* + t_{13}^2 J_{33}^*, \quad G_2 = t_{21}^2 J_{13}^* + t_{21}t_{22}J_{23}^* + t_{21}t_{23}J_{33}^*,\\
H_2 &= t_{21}t_{22}J_{13}^* + t_{22}^2 J_{23}^* + t_{22}t_{23}J_{33}^*, \quad I_2 = t_{21}t_{23}J_{13}^* + t_{22}t_{23}J_{23}^* + t_{23}^2 J_{33}^*,\\
G_3 &= 2t_{11}t_{21}J_{13}^* + t_{21}t_{12}J_{23}^* + t_{11}t_{22}J_{23}^* + t_{21}t_{13}J_{33}^* + t_{11}t_{23}J_{33}^*,\\
H_3 &= t_{21}t_{12}J_{13}^* + t_{11}t_{22}J_{13}^* + 2t_{12}t_{22}J_{23}^* + t_{22}t_{13}J_{33}^* + t_{12}t_{23}J_{33}^*,\\
I_3 &= t_{21}t_{13}J_{13}^* + t_{11}t_{23}J_{13}^* + t_{13}t_{22}J_{23}^* + t_{12}t_{23}J_{23}^* + 2t_{13}t_{23}J_{33}^*,\\
G_4 &= 2t_{21}t_{31}J_{13}^* + t_{31}t_{22}J_{23}^* + t_{21}t_{32}J_{23}^* + t_{31}t_{23}J_{33}^* + t_{21}t_{33}J_{33}^*,\\
H_4 &= t_{31}t_{22}J_{13}^* + t_{21}t_{32}J_{13}^* + 2t_{22}t_{32}J_{23}^* + t_{32}t_{23}J_{33}^* + t_{22}t_{33}J_{33}^*,\\
I_4 &= t_{31}t_{23}J_{13}^* + t_{21}t_{33}J_{13}^* + t_{23}t_{32}J_{23}^* + t_{22}t_{33}J_{23}^* + 2t_{23}t_{33}J_{33}^*,\\
G_5 &= 2t_{31}t_{11}J_{13}^* + t_{31}t_{12}J_{23}^* + t_{11}t_{32}J_{23}^* + t_{31}t_{13}J_{33}^* + t_{11}t_{33}J_{33}^*,\\
H_5 &= t_{31}t_{12}J_{13}^* + t_{11}t_{32}J_{13}^* + 2t_{12}t_{32}J_{23}^* + t_{32}t_{13}J_{33}^* + t_{12}t_{33}J_{33}^*,\\
I_5 &= t_{31}t_{13}J_{13}^* + t_{11}t_{33}J_{13}^* + t_{32}t_{13}J_{23}^* + t_{12}t_{33}J_{23}^* + 2t_{13}t_{33}J_{33}^*,\\
G_6 &= t_{31}^2 J_{13}^* + t_{31}t_{32}J_{23}^* + t_{31}t_{33}J_{33}^*, H_6 = t_{31}t_{32}J_{13}^* + t_{32}^2 J_{23}^* + t_{32}t_{33}J_{33}^*,\\
I_6 &= t_{31}t_{33}J_{13}^* + t_{32}t_{33}J_{23}^* + t_{33}^2 J_{33}^*.
\end{aligned}
$$

$$
\begin{array}{lll}
A'_1 = t_{11}A_1 + t_{12}C_1 + t_{13}E_1, & B'_1 = t_{11}B_1 + t_{12}D_1 + t_{13}F_1, & C'_1 = t_{21}A_1 + t_{22}C_1 + t_{23}E_1,\\
D'_1 = t_{21}B_1 + t_{22}D_1 + t_{23}F_1, & E'_1 = t_{31}A_1 + t_{32}C_1 + t_{33}E_1, & F'_1 = t_{31}B_1 + t_{32}D_1 + t_{33}F_1,\\
G'_1 = t_{11}G_1 + t_{12}H_1 + t_{13}I_1, & H'_1 = t_{21}G_1 + t_{22}H_1 + t_{23}I_1, & I'_1 = t_{31}G_1 + t_{32}H_1 + t_{33}I_1,\\
A'_2 = t_{11}A_2 + t_{12}C_2 + t_{13}E_2, & B'_2 = t_{11}B_2 + t_{12}D_2 + t_{13}F_2, & C'_2 = t_{21}A_2 + t_{22}C_2 + t_{23}E_2,\\
D'_2 = t_{21}B_2 + t_{22}D_2 + t_{23}F_2, & E'_2 = t_{31}A_2 + t_{32}C_2 + t_{33}E_2, & F'_2 = t_{31}B_2 + t_{32}D_2 + t_{33}F_2,\\
G'_2 = t_{11}G_2 + t_{12}H_2 + t_{13}I_2, & H'_2 = t_{21}G_2 + t_{22}H_2 + t_{23}I_2, & I'_2 = t_{31}G_2 + t_{32}H_2 + t_{33}I_2,\\
A'_3 = t_{11}A_3 + t_{12}C_3 + t_{13}E_3, & B'_3 = t_{11}B_3 + t_{12}D_3 + t_{13}F_3, & C'_3 = t_{21}A_3 + t_{22}C_3 + t_{23}E_3,\\
D'_3 = t_{21}B_3 + t_{22}D_3 + t_{23}F_3, & E'_3 = t_{31}A_3 + t_{32}C_3 + t_{33}E_3, & F'_3 = t_{31}B_3 + t_{32}D_3 + t_{33}F_3,\\
G'_3 = t_{11}G_3 + t_{12}H_3 + t_{13}I_3, & H'_3 = t_{21}G_3 + t_{22}H_3 + t_{23}I_3, & I'_3 = t_{31}G_3 + t_{32}H_3 + t_{33}I_3,\\
A'_4 = t_{11}A_4 + t_{12}C_4 + t_{13}E_4, & B'_4 = t_{11}B_4 + t_{12}D_4 + t_{13}F_4, & C'_4 = t_{21}A_4 + t_{22}C_4 + t_{23}E_4,\\
D'_4 = t_{21}B_4 + t_{22}D_4 + t_{23}F_4, & E'_4 = t_{31}A_4 + t_{32}C_4 + t_{33}E_4, & F'_4 = t_{31}B_4 + t_{32}D_4 + t_{33}F_4,\\
G'_4 = t_{11}G_4 + t_{12}H_4 + t_{13}I_4, & H'_4 = t_{21}G_4 + t_{22}H_4 + t_{23}I_4, & I'_4 = t_{31}G_4 + t_{32}H_4 + t_{33}I_4,\\
A'_5 = t_{11}A_5 + t_{12}C_5 + t_{13}E_5, & B'_5 = t_{11}B_5 + t_{12}D_5 + t_{13}F_5, & C'_5 = t_{21}A_5 + t_{22}C_5 + t_{23}E_5,\\
D'_5 = t_{21}B_5 + t_{22}D_5 + t_{23}F_5, & E'_5 = t_{31}A_5 + t_{32}C_5 + t_{33}E_5, & F'_5 = t_{31}B_5 + t_{32}D_5 + t_{33}F_5,\\
G'_5 = t_{11}G_5 + t_{12}H_5 + t_{13}I_5, & H'_5 = t_{21}G_5 + t_{22}H_5 + t_{23}I_5, & I'_5 = t_{31}G_5 + t_{32}H_5 + t_{33}I_5,\\
A'_6 = t_{11}A_6 + t_{12}C_6 + t_{13}E_6, & B'_6 = t_{11}B_6 + t_{12}D_6 + t_{13}F_6, & C'_6 = t_{21}A_6 + t_{22}C_6 + t_{23}E_6,\\
D'_6 = t_{21}B_6 + t_{22}D_6 + t_{23}F_6, & E'_6 = t_{31}A_6 + t_{32}C_6 + t_{33}E_6, & F'_6 = t_{31}B_6 + t_{32}D_6 + t_{33}F_6,\\
G'_6 = t_{11}G_6 + t_{12}H_6 + t_{13}I_6, & H'_6 = t_{21}G_6 + t_{22}H_6 + t_{23}I_6, & I'_6 = t_{31}G_6 + t_{32}H_6 + t_{33}I_6.
\end{array}
$$

Appendix B

$$
\begin{array}{l}
C\xi_{I_1}(\xi,\eta) = \frac{1}{4}\left(-\eta - \sqrt{3}\xi\right)(1-\eta), \quad C\xi_{I_2}(\xi,\eta) = \frac{1}{4}\left(-\eta + \sqrt{3}\xi\right)(1-\eta), \quad C\xi_{I_3}(\xi,\eta) = \frac{1}{4}\left(\eta + \sqrt{3}\xi\right)(1+\eta),\\
C\xi_{I_4}(\xi,\eta) = \frac{1}{4}\left(\eta - \sqrt{3}\xi\right)(1+\eta), \quad C\xi_{I_5}(\xi,\eta) = 1-\eta^2,\\
C\eta_{J_1}(\xi,\eta) = \frac{1}{4}\left(-\xi - \sqrt{3}\eta\right)(1-\xi), \quad C\eta_{J_2}(\xi,\eta) = \frac{1}{4}\left(\xi - \sqrt{3}\eta\right)(1+\xi), \quad C\eta_{J_3}(\xi,\eta) = \frac{1}{4}\left(\xi + \sqrt{3}\eta\right)(1+\xi),\\
C\eta_{J_4}(\xi,\eta) = \frac{1}{4}\left(-\xi + \sqrt{3}\eta\right)(1-\xi), \quad C\eta_{J_5}(\xi,\eta) = 1-\xi^2,\\
C\xi\eta_{M_1}(\xi,\eta) = \frac{1}{4}\left(1 - \sqrt{3}\xi\right)\left(1 - \sqrt{3}\eta\right), \quad C\xi\eta_{M_2}(\xi,\eta) = \frac{1}{4}\left(1 + \sqrt{3}\xi\right)\left(1 - \sqrt{3}\eta\right),\\
C\xi\eta_{M_3}(\xi,\eta) = \frac{1}{4}\left(1 + \sqrt{3}\xi\right)\left(1 + \sqrt{3}\eta\right), \quad C\xi\eta_{M_4}(\xi,\eta) = \frac{1}{4}\left(1 - \sqrt{3}\xi\right)\left(1 + \sqrt{3}\eta\right).
\end{array}
$$

References

Afonso, S.M.B., Hinton, E., 1995. Free vibration analysis and shape optimization of variable thickness plates and shells-I. Finite element studies. Computing Systems in Engineering 6, 27–45.

Babuska, I., Li, L., 1991. Hierarchic modeling of plates. Computers and Structures 40, 419–430.

Batoz, J.L., Dhatt, G., 1992. Modélisation des Structures par Éléments Finis. Coques, Hérmes, Paris, France.

Batoz, J.L., Hammadi, F., Zheng, C., Zhong, W., 2000. On the linear analysis of plates and shells using a new-16 degrees of freedom flat shell element. Computers and Structures 78, 11–20.

Bhaskar, K., Kaushik, B., 2004. Simple and exact series solutions for flexure of orthotropic rectangular plates with any combination of clamped and simply supported edges. Composite Structures 63, 63–68.

Bischoff, M., Ramm, E., 1997. Shear deformation shell elements for large strains and rotations. International Journal for Numerical Methods in Engineering 40, 4427–4449.

Bischoff, M., Ramm, E., 2000. On the physical significance of higher order kinematic and static variables in a three-dimensional shell formulation. International Journal of Solids and Structures 37, 6933–6960.

Bischoff, M., Wall, W.A., Bletzinger, K.-U., Ramm, E., 2004. Models and finite elements for thin-walled structures. In: Stein, Erwin, Borst, René de, Hughes, Thomas J.R. (Eds.), Encyclopedia of Computational Mechanics. Solids and Structures, vol. 2. John Wiley & Sons, Ltd, Chichester, pp. 59–137.

Bouabdallah, M.S., Batoz, J.L., 1996. Formulation and evaluation of a finite element model for the linear analysis of stiffened composite cylindrical panels. Finite Elements in Analysis and Design 21, 265–289.

Büchter, N., Ramm, E., 1992. 3D-extension of nonlinear shell equations based on the enhanced assumed strain concept. In: Hirsch, C. (Ed.), Computational Methods in Applied Sciences. Elsevier, Amsterdam, pp. 55–62.

Büchter, N., Ramm, E., Roehl, D., 1994. Three-dimensional extension of non-linear shell formulation based on the enhanced assumed strain concept. International Journal for Numerical Methods in Engineering 37, 2551–2568.

Carrera, E., Brischetto, S., 2008a. Analysis of thickness locking in classical, refined and mixed multilayered plate theories. Composite Structures 82, 549–562.

Carrera, E., Brischetto, S., 2008b. Analysis of thickness locking in classical, refined and mixed theories for layered shells. Composite Structures 85, 83–90.

Carrera, E., 2002. Theories and finite elements for multilayered anisotropic, composite plates and shells. Archives of Computational Methods in Engineering 9, 87–140.

Carrera, E., 2003. Theories and finite elements for multilayered plates and shells: a unified compact formulation with numerical assessment and benchmarking. Archives of Computational Methods in Engineering 10, 215–296.

Chapelle, D., Bathe, K.-J., 1998. Fundamental considerations for the finite element analysis of shell structures. Computers and Structures 66, 19–36.

Chapelle, D., Oliveira, D.L., Bucalem, M.L., 2003. MITC elements for a classical shell model. Computers and Structures 81, 523–533.

Cho, M., Roh, H.Y., 2003. Development of geometrically exact new elements based on general curvilinear coordinates. International Journal for Numerical Methods in Engineering 56, 81–115.

Dau, F., Polit, O., Touratier, M., 2004. An efficient C1 finite element with continuity requirements for multilayered/sandwich shell structures. Computers and Structures 82, 1889–1899.

Dau, F., Polit, O., Touratier, M., 2006. C1 plate and shell finite elements for geometrically nonlinear analysis of multilayered structures. Computers and Structures 84, 1264–1274.

Flügge, W., 1973. Stresses in Shells. Springer-Verlag, Berlin, Germany.

Heppler, G.R., Hansen, J.S., 1986. A mindlin element for thick and deep shells. Computer Methods in Applied Mechanics and Engineering 54, 21–47.

Huang, H.C., Hinton, E., 1986. A new nine node degenerated shell element with enhanced membrane and shear interpolation. International Journal for Numerical Methods in Engineering 22, 73–92.

Jones, I.A., 2002. Pinched cylinder benchmarks for shear deformable laminated shells. Plastics, Rubber and Composites 31, 249–261.

Kirchhoff, G., 1850. Über das Gleichgewicht und die Bewegung einer elastischen Scheibe. Journal für die Reine und Angewandte Math 40, 51–88.

Kulikov, G.M., Carrera, E., 2008. Finite element higher-order shell models and rigid-body motions. International Journal of Solids and Structures 45, 3153–3172.

Kulikov, G.M., Plotnikova, S.V., 2002. Simple and effective elements based upon Timoshenko-Mindlin shell theory. Computer Methods in Applied Mechanics and Engineering 191, 1173–1187.

Kulikov, G.M., 2001. Refined global approximation theory of multilayered plates and shells. Journal of Engineering Mechanics 127, 119–125.

Lee, P.-H., Bathe, K.-J., 2005. Insight into finite element shell discretizations by use of the "basic shell mathematical model". Computers and Structures 83, 69–90.

MacNeal, R.H., 1998. Perspective on finite elements for shell analysis. Finite Elements in Analysis and Design 30, 175–186.

Mindlin, R.D., 1951. Influence of rotatory inertia and shear on flexural motions of isotropic, elastic plates. Journal of Applied Mechanics 18, 31–38.

Parisch, H., 1979. A critical survey of the 9-node degenerated shell element with special emphasis on thin shell application and reduced integration. Computer Methods in Applied Mechanics and Engineering 20, 323–350.
Parisch, H., 1995. A continuum-based shell theory for non-linear applications. International Journal for Numerical Methods in Engineering 38, 1855–1883.
Polit, O., 1992. Développement d' éléments Finis de Plaque Semi-épaisse et de Coque Semi-épaisse a Double Courbure, Thése de doctorat (PhD Thesis), Université Paris VI.
Polit, O., 2008. Modéle de Coque et Approche Dégénérée, Internal Report. In: Laboratoire Energétique Mécanique Electromagnétisme. Université Paris Ouest Nanterre La Défense, Paris, France.
Ramm, E., 1986. Form und Tragverhalten. In: Ramm, E., Schunck, E. (Eds.), Heinz Isler Schalen. Karl Krämer Verlag, Stuttgart, pp. 29–34.
Reddy, J.N., 1984. A simple higher-order theories for laminated composite plates. Journal of Applied Mechanics 51, 745–752.
Reddy, J.N., 2004. Mechanics of Laminated Composite Plates and Shells. Theory and Analysis. CRC Press, Boca Raton, Florida (USA).
Reissner, E., 1945. The effect of transverse shear deformation on the bending of elastic plates. Journal of Applied Mechanics 12, 69–77.
Ren, J.G., 1987. Exact solutions for laminated cylindrical shells in cylindrical bending. Composite Science and Technology 29, 169–187.
Sanders, J.L., 1959. An Improved First Approximation Theory for Thin shells, NASA report R24.
Touratier, M., Faye, J.-P., 1995. On a refined model in structural mechanics: finite element approximation and edge effect analysis for axisymmetric shells. Computers and Structures 54, 897–920.
Vu-Quoc, L., Tan, X.G., 2003. Optimal solid shells for non-linear analyses of multilayer composites. I. Statics. Computer Methods in Applied Mechanics and Engineering 192, 975–1016.
Zhao, X., Liu, G.R., Dai, K.Y., Zhong, Z.H., Li, G.Y., Han, X., 2008. Geometric nonlinear analysis of plates and cylindrical shells via a linearly conforming radial point interpolation method. Computational Mechanics 42, 133–144.
Zienkiewicz, O.C., Taylor, R.L., 2005. The Finite Element Method for Solid and Structural Mechanics. Elsevier Ltd, Oxford, UK.